

1 Large-Scale Biology article

2

3 **The systems architecture of molecular memory in poplar after abiotic stress**

4

5 Elisabeth Georgii¹, Karl Kugler², Matthias Pfeifer², Elisa Vanzo³, Katja Block³, Malgorzata A.
6 Domagalska⁴, Werner Jud^{3,6}, Hamada AbdElgawad⁴, Han Asard⁴, Richard Reinhardt⁵, Armin
7 Hansel⁶, Manuel Spannagl², Anton R. Schäffner¹, Klaus Palme⁷, Klaus F.X. Mayer^{2,8*}, Jörg-
8 Peter Schnitzler^{3*}

9

10 ¹ Institute of Biochemical Plant Pathology, Helmholtz Zentrum München, German Research
11 Center for Environmental Health, 85764 Neuherberg, Germany.

12 ² Plant Genome and Systems Biology, Helmholtz Zentrum München, German Research
13 Center for Environmental Health, 85764 Neuherberg, Germany.

14 ³ Research Unit Environmental Simulation, Helmholtz Zentrum München, German Research
15 Center for Environmental Health, 85764 Neuherberg, Germany.

16 ⁴ Laboratory for Integrated Molecular Plant Research, University of Antwerp, 2020 Antwerp,
17 Belgium.

18 ⁵ Max Planck Genome Centre Cologne, Max Planck Institute for Plant Breeding Research,
19 50829 Köln, Germany.

20 ⁶ Institute for Ion Physics and Applied Physics, University of Innsbruck, 6020 Innsbruck,
21 Austria.

22 ⁷ Institute of Biology II/Molecular Plant Physiology, Faculty of Biology, BIOS Centre for
23 Biological Signalling Studies, Centre for Biological Systems Analysis, 79104 Freiburg,
24 Germany.

25 ⁸ TUM School of Life Sciences, Technical University Munich, Weihenstephan, Germany.

26

27 * Corresponding authors:

28 Jörg-Peter Schnitzler, Tel: +49-89-31872413, jp.schnitzler@helmholtz-muenchen.de;

29 Klaus F.X. Mayer, Tel: +49-89-31873584, k.mayer@helmholtz-muenchen.de.

30

31

32

33

34 **Title: The systems architecture of molecular memory in poplar after abiotic stress**

35 **Short title: Systems architecture of molecular memory**

36

37 The author responsible for distribution of materials integral to the findings presented in this
38 article in accordance with the policy described in the Instructions for Authors
39 (www.plantcell.org) is: Jörg-Peter Schnitzler (jp.schnitzler@helmholtz-muenchen.de).

40 **ABSTRACT**

41

42 Throughout the temperate zones, plants face combined drought and heat spells in increasing
43 frequency and intensity. We compared periodic (intermittent, i.e. high-frequency) versus
44 chronic (continuous, i.e. high-intensity) drought-heat stress scenarios in Gray poplar (*Populus*
45 *x canescens*) plants for phenotypic and transcriptomic effects during stress and recovery.
46 Post-recovery photosynthetic productivity after stress exceeded the performance of poplar
47 trees without stress experience. We analyzed the molecular basis of this stress-related
48 memory phenotype and investigated gene expression responses across five major tree
49 compartments including organs and wood tissues. For each of these tissue samples,
50 transcriptomic changes induced by the two stress scenarios were highly similar during the
51 stress phase but strikingly divergent after recovery. Characteristic molecular response
52 patterns were found across tissues but involved different genes in each tissue. Only a small
53 fraction of genes showed similar stress and recovery expression profiles across all tissues,
54 among them protein phosphatases of type 2C, the LATE EMBRYOGENESIS ABUNDANT
55 PROTEIN 4-5 genes and orthologs to the *Arabidopsis thaliana* transcription factor
56 HOMEBOX LEUCINE-ZIPPER PROTEIN 7. Predicted transcription factor regulatory
57 networks for these genes suggest that a complex interplay of common and tissue-specific
58 components contributes to the coordination of post-recovery responses to stress in woody
59 plants.

60

61

62 **INTRODUCTION**

63

64 Climate change increases the frequency and intensity of extreme events such as heat waves
65 and drought (IPCC, 2014). Plants, as sessile organisms, and in particular long-living trees,
66 have evolved flexible mechanisms to cope with environmental stresses (Harfouche et al.,
67 2014). Poplar is a widely used model in tree research that combines moderate genome size,
68 a complete genome reference, fast growth, rapid maturation and wide geographic distribution
69 with economic relevance in wood and biomass production (Taylor, 2002; Tuskan et al., 2006).
70 It is also suitable for transcriptome studies across a variety of tissues. For instance, co-
71 expression patterns underlying cambial growth and wood formation have been investigated
72 by sampling multiple sections across tree trunks (Sundell et al., 2017). Various physiological

73 changes have been observed in plants in response to abiotic stresses. Drought limits the root
74 water uptake and results in a reduction of transpiration and photosynthesis, which can have
75 severe effects on growth and yield (Aroca et al., 2012; Osakabe et al., 2014). These
76 processes are mediated by well-known molecular responses of cells to drought, frequently
77 triggered by the plant hormone abscisic acid (ABA) (Osakabe et al., 2014; Shinozaki and
78 Yamaguchi-Shinozaki, 2007). In addition to ABA-responsive element-binding (AREB/ABF)
79 transcription factors, members of the no apical meristem, Arabidopsis transcription activation
80 factor and cup-shaped cotyledon (NAC) and dehydration-responsive element-binding (DREB)
81 transcription factor families orchestrate pronounced gene expression changes upon drought
82 stress, as demonstrated in Arabidopsis and crop species (Nakashima et al., 2014).

83 Stress exposure alters gene expression also beyond the duration of the stress phase, forming
84 a molecular "memory" (Crisp et al., 2016; Fleita-Soriano and Munne-Bosch, 2016). A well-
85 studied effect of stress-related memory is enhanced tolerance towards subsequent stress
86 events, reflected by response differences between the first and subsequent stress challenges
87 (Ding et al., 2012; Ding et al., 2013; Liu et al., 2016). This "primed response" is characterized
88 by gene expression changes inducing damage protection, growth regulation, osmotic
89 readjustment and coordination of hormone crosstalk (Ding et al., 2013). Such an expression
90 memory can also involve chromatin remodeling through histone modifications (Lämke et al.,
91 2016; Sani et al., 2013). Phenotypically, plants primed by drought stress have shown a higher
92 photosynthesis rate during subsequent stress periods than non-primed plants (Wang et al.,
93 2014). Even in the absence of a further stress challenge, plant performance can have signs of
94 a stress-related memory after successful stress recovery, significantly differing from untreated
95 control plants (Hagedorn et al., 2016; Xu et al., 2010). The molecular basis of this post-
96 recovery phenotype is still largely unexplored. The present study focuses on gene expression
97 changes during stress and after recovery in a woody plant species. In particular, we
98 investigated expression characteristics of stress-related memory, which we define in the
99 context of this work as a post-recovery steady state in stress-treated trees that is distinct from
100 non-treated trees. Our analysis not only contrasts stress scenarios that differ in frequency and
101 intensity but also compares responses in different tissues of poplar trees.

102 Simulating predicted regional climate conditions (IPCC, 2014) by applying simultaneous
103 drought and heat spells at elevated atmospheric carbon dioxide (CO₂) concentrations
104 expected in 2050, we explored how Gray poplars (*Populus x canescens*) that have recovered

105 from drought-heat stress differ from non-treated plants. We characterized the stress response
106 and the stress-related post-recovery memory regarding leaf photosynthesis phenotypes and
107 transcriptional responses of young (“sink”) and mature (“source”) leaves (Vanzo et al., 2015),
108 phloem-bark, developing xylem and roots. Two stress scenarios of equal total duration were
109 compared to contrast periodic, intermittent stress (PS) with chronic, continuous stress (CS).

110 The post-recovery effects of abiotic stress we observed at the transcriptome level extend the
111 so far established concept of a molecular memory after stress exposure. While previous work
112 has analyzed gene expression changes in response to recurrent versus initial stress
113 challenges, our analysis additionally investigates stress-induced shifts in steady state after
114 recovery, i.e., before a new stress challenge. Still, the aspect of recurrent versus one-time
115 stress is covered by the two stress scenarios, which are compared to control scenarios not
116 only at the end of the stress phase but also after recovery. The multifactorial study sheds new
117 light on the regulatory architecture of memory-related gene expression networks after
118 different climatic challenges and across multiple tree organs and tissues.

119

120 **RESULTS**

121

122 **Impact of drought-heat stress periods on post-recovery photosynthetic performance**

123 To get a systems level view on stress response and recovery in a woody plant species, we
124 subjected groups of Gray poplar (*Populus x canescens*) trees to one of four climate scenarios
125 and collected transcriptome samples from five tree compartments (organs and wood tissues)
126 at two subsequent time points (Fig. 1). In addition, phenotypic measurements of leaf
127 photosynthesis were recorded on attached leaves (Fig. 1A). The experiment was performed
128 in climate chambers under highly controlled conditions, including a chronic drought and heat
129 stress scenario at elevated CO₂ levels (CS scenario), a periodic drought and heat stress
130 scenario at elevated CO₂ levels with two intermediate recovery periods (PS scenario), a
131 control scenario at elevated CO₂ levels (EC scenario) and a control scenario at ambient CO₂
132 levels (AC scenario) (Vanzo et al., 2015). AC represents the current temperate climate as a
133 reference point, which allowed us to estimate the effects of predicted future climate scenarios
134 (EC, CS and PS). The stress phase of 22 days was followed by a recovery period of one

135 week at irrigation and temperature conditions that were equal to those for control plants
136 (Methods). Phenotypic photosynthetic performance of mature leaves was assessed using gas
137 exchange measurements (Jud et al., 2016; Vanzo et al., 2015). During the stress phase, the
138 net CO₂ assimilation rate of leaves was significantly decreased for CS-treated poplar trees
139 compared to the corresponding EC control trees (p.adj=0.0347). PS-treated trees showed
140 intermediate levels (Fig. 1B). The same response pattern was found for the transpiration rate
141 (Fig. 1C) and stomatal conductance (Fig. 1D). For all three physiological parameters, AC and
142 EC controls were not significantly different. At the end of the recovery phase, the leaf
143 transpiration rate and stomatal conductance of stress-treated trees reached similar levels as
144 for the control trees, suggesting that the trees indeed had recovered from the combined
145 drought and heat spells (Fig. 1C-D). The recovery of the physiological phenotype is also
146 confirmed by the clear separation between stress phase and recovery measurements for
147 each stress treatment and physiological parameter (Fig. 1B-D). Remarkably, the leaf net CO₂
148 assimilation rate of PS- and CS-treated trees was not only recovered but significantly higher
149 than in AC trees (p.adj=0.0089 and p.adj=0.0388, respectively), with intermediate levels for
150 EC trees (Fig. 1B). Evaluating continuous net ecosystem exchange measurements
151 throughout the entire experiment (Vanzo et al., 2015), both PS- and CS-treatments led to a
152 significant increase of the daily rates of canopy level C gain from photosynthesis during the
153 second half of the recovery phase (days 26 to 29), in comparison with the control scenarios
154 (Fig. 1E).

155

156 **Shared effects between transcriptomic and phenotypic data**

157 We integrated photosynthetic gas exchange data with RNA-seq data of mature leaves by
158 regularized canonical correlation analysis (Le Cao et al., 2009) (Methods). RNA-seq reads
159 were mapped to the *Populus trichocarpa* reference genome (Sundell et al., 2017; Tuskan et
160 al., 2006). Both data types shared major stress and recovery effects, reflected by the first and
161 second correlated component, respectively (Fig. 1F). For component one, the most
162 representative phenotypic variable is the ratio between net CO₂ assimilation rate and stomatal
163 conductance (Pearson correlation -0.96). The leaf transpiration rate showed a correlation of
164 0.95 with component one, consistent with the stomatal closure upon drought stress (Osakabe
165 et al., 2014). The dominating genes for component one also have known stress response

166 functions. Among the top ten genes up-regulated in stress (correlation < -0.95), six genes
167 were annotated as heat shock proteins (Potri.012G022400, Potri.010G195700,
168 Potri.013G089200, Potri.017G130700, Potri.010G088600, Potri.010G053400), potentially
169 acting as chaperones in protein folding. This could indicate a response to elevated leaf
170 temperature caused by heat and lack of transpiration cooling (Kotak et al., 2007). Indeed, the
171 mean temperature of mature leaves in the experiment increased to more than 35°C during PS
172 and CS, whereas it ranged between 27°C and 30°C after recovery and for controls (see Fig.
173 S4 of Vanzo et al., 2015). Considering all 589 genes that were up-regulated under PS and CS
174 in mature leaves ($\log_2(\text{fold change}) > 1$, $p.\text{adj} < 0.05$; Table S1), protein folding is also the top
175 enriched Gene Ontology (GO) category ($p.\text{adj} = 5.64e-9$; Table S2). At the same time, the top
176 down-regulated variables associated with component one included a MYB (myeloblastosis)
177 transcription factor (Potri.002G260000), a peroxidase (Potri.016G132666) and a glutaredoxin
178 gene (Potri.014G134300), indicating changes in transcriptional regulation and stress
179 signaling. Oxidoreductase, peroxidase and transcription factor activity functions were also
180 significantly enriched among the genes down-regulated in mature leaves by both stresses,
181 and along with them many other processes including protein phosphorylation, cell wall
182 modification, proteolysis, transmembrane transport, cell division and defense response (Table
183 S3). The recovery phase mature leaf samples are indistinguishable from control samples with
184 respect to component one, suggesting the disappearance of major stress characteristics and
185 thus successful recovery.

186 The second component linking phenotypic and gene expression data points to differences
187 between recovery phase samples and untreated samples (Fig. 1F). Component two is
188 characterized by an increased mean net CO₂ assimilation rate in the recovery samples
189 (Pearson correlation 0.77), consistent with the phenotypic data analysis (Fig. 1B). Individual
190 genes did not correlate significantly with component two, and the up-regulated genes shared
191 by both stress treatments after recovery were not enriched for specific functions (Table S4).
192 Nucleotide binding and ATPase activity for transmembrane movement were enriched among
193 the down-regulated genes of both stress treatments but much more pronounced for CS
194 (Table S5). PS-specific up-regulation was enriched for stress response genes (e.g. the heat
195 shock protein Potri.004G073600, Table S4). Many genes were up-regulated only for one
196 stress treatment type, for instance the putatively photosynthesis-associated plastocyanin-like
197 domain gene Potri.001G332200 was only up-regulated for PS (Table S1, Fig. 2). This

198 indicates that post-recovery transcriptomes of PS and CS in mature leaves share more
199 subtle, multivariate effects.

200

201 **Systemic and tissue-specific stress responses**

202 In addition to the mature leaf data described so far, we also obtained RNA-seq
203 measurements from young leaves, phloem-bark, developing xylem and fine roots. This
204 provides a comprehensive systems-level view on the transcriptional responses occurring
205 during stress application and after recovery (Fig. 2). To simplify figure keys and description,
206 the term "tissue" hereafter refers to exactly this set of organs and tissues. The predominant
207 gene expression variation across biological samples was attributable to distinct tissue
208 characteristics (Fig. 2A). Whole-tree gene expression profiles concatenating profiles of tissue
209 samples from the same tree clearly separate PS and CS stress phase trees from controls and
210 recovery phase trees (Fig. 2B). In all tissues, PS and CS evoked very similar transcriptomic
211 responses relative to EC. Both for up- and down-regulated genes ($\text{abs}(\log_2 \text{ fold change}) > 1$,
212 $p.\text{adj} < 0.05$), the observed overlap between the stress types was always larger than one or
213 both of the stress type-specific fractions, suggesting that both scenarios evoke similar
214 molecular stress responses in the tree (Fig. 2C, top panel). Among all tissues, the largest
215 overlap between the two stress types was found in the developing xylem, indicating
216 pronounced changes in the upward transport system of the plant. Significantly enriched GO
217 functions ($p.\text{adj} < 0.05$) among the up-regulated genes that overlap between PS and CS xylem
218 samples include oxidoreductase activity, transcription factor activity, transporter activity and
219 response to stress. In the root, genes encoding recognition proteins (e.g. lectin, glycoprotein)
220 and ATPases were activated by both stress types, whereas common stress responses in
221 phloem-bark and leaves were dominated by protein folding processes (Table S2). In total
222 three genes were found to be up-regulated for each stress scenario in each tissue:
223 Potri.T044100 (one of two co-orthologs of the TCP (TEOSINTE BRANCHED 1, CYCLOIDEA,
224 PCF) family transcription factors AT5G41030 and AT3G27010), Potri.008G133200 (one of
225 two co-orthologs of the O-glycosyl hydrolase AT2G01630) and Potri.001G293000 (not
226 annotated).

227 Regarding the down-regulated genes in both stress types, the developing xylem showed
228 many enriched processes, such as translation, microtubule-based movement, DNA

229 replication, carbohydrate metabolic process, cell wall, electron transfer activity and
230 transmembrane transport, suggesting a down-regulation of cell division and growth (Table
231 S3). Similarly, roots showed significant down-regulation of nucleosome, cell wall, electron
232 transfer activity and carbohydrate metabolic process genes. For phloem-bark we also
233 observed a significant transcriptional decrease of cell wall modification, microtubule-based
234 movement and carbohydrate metabolic process. In addition, a strong reduction of proteolysis
235 and response to oxidative stress was found in this tissue. The same was observed for down-
236 regulated genes in young leaves, with an additional enrichment in fatty acid biosynthetic
237 process, transmembrane transport, DNA replication and response to auxin. Along with the
238 observations in mature leaves (see above), we can conclude that both stress treatments, CS
239 as well as PS, had similar effects, leading to down-regulation of growth-related processes
240 across all tissues.

241 However, we also found differences between PS and CS. In leaf and root tissues, PS induced
242 more gene expression changes than CS, whereas the CS response was more pronounced
243 than the PS response in xylem and phloem-bark tissues. The PS-specific up-regulated genes
244 detected in root are enriched for ATPases acting as transporters. This up-regulation might be
245 at least partially attributable to priming effects, since PS plants had experienced their third
246 stress phase whereas CS plants were still in their first stress challenge at d22 (Fig. 1A). CS-
247 specific up-regulated genes in developing xylem are enriched for ATPase activity and
248 photosystem II functions. This gene expression up-regulation is consistent with previous
249 observations that stem photosynthesis using internal CO₂ from respiration may play a role in
250 young poplar plants especially during drought stress (Bloemen et al., 2016), although light
251 penetration through the bark is limited (Pfanz et al., 2002). The CS-specific up-regulation of
252 photosystem genes may reflect the slightly more severe water deficiency during CS (shoot
253 midday water potential (ψ_{md}) -1.52 ± 0.10 MPa) relative to PS (ψ_{md} -1.27 ± 0.05 MPa) and
254 controls (EC: ψ_{md} -0.97 ± 0.07 MPa, AC: -0.97 ± 0.04 MPa), increasing the need for C
255 assimilation via a pathway that does not lead to further dehydration promoted by open
256 stomata. CS-specific down-regulated genes in developing xylem are enriched for
257 endoplasmic reticulum and intracellular protein transport (Table S3). The gene regulations
258 in the developing xylem illustrate the tissue specificity of stress responses, with a high
259 similarity between periodic and chronic stress as well as stress-specific enhancement of
260 processes.

262 Post-recovery characteristics of stress-treated trees

263 After one week of recovery from the periodic or chronic stress, respectively, the total number
264 of differentially regulated genes relative to the EC control plants was lower than at the end of
265 the stress phase across all poplar tissues (Fig. 2C). This suggests that the transcriptomes
266 had left the stress state and approached the state of control plants again. The stress recovery
267 was physiologically confirmed by measurements of gas exchange (Fig. 1C-D) and shoot
268 water potentials, which had recovered to -0.72 ± 0.10 MPa and -0.93 ± 0.07 MPa in PS and CS,
269 respectively (compare previous paragraph, Methods). In contrast to the stress phase
270 observations, fewer differentially expressed genes were shared between PS and CS than
271 were specifically up- or down-regulated in one of the two stress scenarios (Fig. 2C, bottom
272 panel). This divergence between stress types during the recovery phase indicates that most
273 stress-activated genes are no longer induced and that the recurrence or the duration of
274 drought-heat stress alter the post-recovery processes of plants. In all tissues except mature
275 leaves PS induced more recovery-phase up-regulated genes than CS.

276 The largest number of PS up-regulated genes occurred in young (sink) leaves (Vanzo et al.,
277 2015), followed by mature (source) leaves. In young leaves, the gene expression up-
278 regulation at recovery from PS was dominated by oxidation-reduction, coenzyme binding,
279 hexosyl transferase and carbohydrate metabolic process GO terms (Table S4). The re-
280 induction of carbohydrate metabolism gene expression after its decrease during stress (see
281 above) indicates the reactivation of growth processes in young leaves. CS-specific expression
282 patterns were characterized by a down-regulation of genes involved in unfolded protein
283 binding, protein folding and response to stress for young leaves and down-regulation of
284 oxidoreductase activity for phloem, indicative of stress recovery (Table S5). In contrast, for
285 post-recovery mature leaves, PS-specific enrichment indicated continued activity of several
286 stress response genes, e.g. with functions as heat shock protein (Potri.004G073600) or
287 drought-related late embryogenesis abundant protein (Potri.010G012100). Also transcription
288 factors showed a PS-specific transcriptional up-regulation in post-recovery mature leaves,
289 e.g. Potri.006G221500, one of six poplar co-orthologs of Arabidopsis MYB123 involved in
290 anthocyanin and pro-anthocyanidin biosynthesis. In agreement with that, anthocyanin levels
291 of poplar leaves at the post-recovery time point were higher for PS than for EC and CS

292 (Vanzo et al., 2015). Transporter activity tended to be up-regulated in young leaves
293 (p.adj=0.06) including many aquaporin genes (Potri.001G235300, Potri.009G005400,
294 Potri.009G013900, Potri.009G027200), some of which were also up-regulated in other post-
295 recovery tissues (phloem, mature leaves) of PS or CS trees and could be an indication of
296 drought decline (Table S1).

297 Biochemical data that monitored the antioxidative system in mature leaves also confirm the
298 recovery from the stressed state (Table S6), matching the gene expression response profiles
299 (Fig. 2C). Leaves of PS-treated trees exhibited a significant decrease of relative reduced
300 ascorbate content during the stress phase (p.adj=0.0347), indicating increased scavenging of
301 reactive oxygen species (AbdElgawad et al., 2016). In contrast, all stress-treated and control
302 trees displayed similar leaf levels of relative reduced ascorbate at the end of the recovery
303 phase (Fig. 2D). In addition, we compared the treatment-related expression responses
304 between post-recovery and stress-phase tissue samples to assess how much the molecular
305 processes in each tissue differ between the two phases. Interestingly, the fraction of post-
306 recovery up-regulated genes that already showed up-regulation during the stress phase
307 varied widely among tissues, ranging from 58% in xylem to 7% in young leaves for PS and
308 from 69% in xylem to 6% in mature leaves for CS (Fig. 2E). This suggests that for some
309 tissues molecular processes after recovery resemble molecular processes during stress,
310 whereas for other tissues post-recovery and stress responses are largely different. For
311 instance, ATPases and transport functions played a major role in developing xylem during
312 both phases, whereas for young leaves carbohydrate metabolism was down-regulated during
313 stress (both PS and CS) and up-regulated after recovery.

314 Among different tissues, gene expression response patterns showed only little overlap (Fig.
315 3). During the recovery phase, we did not find any differentially expressed gene that
316 responded across all tissues, neither in PS nor in CS. Nevertheless, the five tissues shared
317 similar characteristic stress and post-recovery expression profiles that involved distinct co-
318 expression modules in each tissue (Fig. 4, Methods, Table S7). Interestingly, more than half
319 of these characteristic profiles exhibited a pronounced difference between stress-exposed
320 plants and non-treated plants at the end of the recovery phase, indicative of stress-related
321 memory (Fig. 4, bottom). For example, young and mature leaf modules in the memory
322 community C12 contained the glutathione-S-transferase Potri.019G130566, which protects
323 against oxidative damage, and the esterase Potri.017G062300 with highest similarity to an

324 *Arabidopsis* gene involved in maintaining the integrity of photosynthetic membranes during
325 abiotic stress (Lippold et al., 2012). Only for a small fraction of genes, PS and CS showed
326 similar cross-tissue memory response patterns (Fig. 5A, Fig. 2C). Among the different tissues,
327 the most pronounced agreement was found for young and mature leaves. The observed
328 divergence between PS and CS was not due to the fold change threshold ($\text{abs}(\log_2 \text{fold change}) > 1$); there were very few genes that satisfied the significance threshold ($p.\text{adj} < 0.05$)
329 but not the fold change threshold (Fig. S1). Differences between PS and CS expression levels
330 were consistent with the control-based comparisons (Fig. 5B).

332 The co-analysis of spatially apart tissues allowed insights into the complexity of coordinated
333 whole-plant long-term responses to periodically occurring stress. Strikingly, the stress and
334 recovery profiles of individual genes along the different trees were not conserved across
335 tissues (Fig. 6). Only for 0.2% of the genes, the expression of the same gene correlated well
336 across all tissues (Fig. 6A). The largest number of self-correlated genes was found between
337 young and mature leaves, reflecting functional similarity of these compartments (Fig. 6B).
338 Furthermore, 995 genes were self-correlated between phloem and xylem. Among them,
339 functions in oxidation-reduction processes, carbohydrate and protein metabolic processes as
340 well as transmembrane transport and microtubule-based processes were abundant. The
341 genes with the strongest self-correlation across all tissues included a large proportion of
342 genes that exhibited a significant post-recovery memory pattern in PS (Fig. 6A, Table S1).
343 The top five genes among them were the transcription factors *HOMEBOX-LEUCINE*
344 *ZIPPER PROTEIN 7 (HB7) co-ortholog 1(of4)* (Potri.014G103000) and *HB7 co-ortholog*
345 *3(of4)* (Potri.001G083700) as well as *GLUTAREDOXIN C1 co-ortholog 2(of2)*
346 (Potri.012G082800) and two clade A protein phosphatases of the 2C family (PP2Cs), the
347 *HIGHLY ABA-INDUCED 1 (HAI1)* ortholog (Potri.009G037300) and Potri.001G092100. In
348 *Arabidopsis thaliana*, HB7 is transcriptionally induced by ABA and positively regulates PP2C
349 gene expression (Valdés et al., 2012).

350

351 **Transcription factors associated with stress-related memory**

352 Transcription factors (TFs) are key regulators at the top level of the molecular hierarchy.
353 Since several memory genes showed similar stress and post-recovery responses across all
354 tissues (Fig. 6A), we were interested whether there exist common regulatory mechanisms

355 among different tissues that may play a role in stress-related memory. We used our gene
356 expression data from each tissue to infer regulatory relationships between known TFs
357 (Berardini et al., 2015; Jin et al., 2014) and these 17 self-correlated memory genes, resulting
358 in a gene regulatory network for each tissue (Fig. 7, Methods). Each of these tissue-specific
359 networks has one main connected component or forms a single connected component,
360 indicating that the self-correlated memory genes (Fig. 7A, gray nodes) share common top
361 candidates of regulatory TFs (which were computationally inferred for each gene by choosing
362 the top five expression predictors, Methods). The majority of candidate TFs were tissue-
363 specific (Fig. 7A, white nodes), but a considerable fraction co-occurred across two up to four
364 tissues. In particular, young and mature leaves shared ten candidate TFs. Edges also were
365 shared across tissues, meaning that a specific TF was found in several tissues among the top
366 five candidate regulators for a specific memory gene (Fig. 7A, colored edges; Fig. 7B). A
367 relationship between *HB7 co-ortholog 1(of4)* (Potri.014G103000) and *HB7 co-ortholog 3(of4)*
368 (Potri.001G083700) was predicted in all tissues except mature leaves. In the co-expression
369 analysis, both of them fell into the tissue-specific co-expression modules of community C2,
370 which was characterized by pronounced stress response during PS and CS (Fig. 4, Table
371 S7). After recovery, a significant 20-fold PS up-regulation of *HB7 co-ortholog 3(of4)* gene
372 expression was observed for both xylem and mature leaves as well as a 200-fold PS up-
373 regulation of the *HB7 co-ortholog 1(of4)* gene for the xylem. In contrast, CS trees did not
374 show significant changes in the expression of these genes relative to control trees (Table S1).
375 The two *HB7* TFs were also central in the sense that together they covered all putative
376 targets (non-TF memory genes) of their subnetwork and their removal would disconnect the
377 network into several parts (Fig. 7B). The *HB7* TFs are members of the homeodomain leucine
378 zipper (HDZIP) family. In *Arabidopsis*, *HB7* has been associated with drought stress response
379 as well as reduced cell elongation in leaves and in the inflorescence stem (Hjellström et al.,
380 2003; Söderman et al., 1996). *HB7* has also been identified as a drought stress memory gene
381 that showed a stronger up-regulation at the third stress experience than after a single
382 incidence (Ding et al., 2013). Under non-stress conditions, *HB7* overexpression has been
383 related to an increase in chlorophyll content and photosynthesis rate (Re et al., 2014),
384 consistent with our physiological observations at the recovery phase.

385 The expression of the *HB7 co-ortholog 1(of4)* (Potri.014G103000) gene itself is putatively
386 related to the expression of the TFs Potri.006G138900, which was found to be a co-predictor

387 with Potri.001G083700 for several putative target genes, and Potri.002G125400 (Fig. 7B).
388 Potri.002G125400 is annotated as *ABSCISIC ACID RESPONSIVE ELEMENTS-BINDING*
389 *FACTOR 2 (ABF2) co-ortholog 1(of2)*. Arabidopsis ABF2 is known to enhance drought
390 tolerance (Nakashima et al., 2014). Potri.006G138900 is a member of the ethylene response
391 factor/ APETALA2 (ERF/AP2) TF family. The closest Arabidopsis ortholog in its evolutionary
392 family, PTHR31985:SF77 (Mi et al., 2017), is AT5G21960, which belongs to the DREB
393 subfamily A-5 with established functions in drought stress response (Singh and Laxmi, 2015).
394 In poplar, the Potri.006G138900 gene has been reported to be induced by four different types
395 of osmotic stresses (Yao et al., 2017). In our data, significant up-regulation of this gene was
396 only observed for PS and not for CS. In Arabidopsis, *RELATED TO AP2 1 (RAP2.1)*, a
397 prominent member of the DREB gene subfamily A-5, is also more induced after repeated
398 application of dehydration stress (Ding et al., 2013). RAP2.1 acts as a negative regulator of
399 *RD/COR (RESPONSIVE TO DESICCATION/ COLD-REGULATED)* genes (Dong and Liu,
400 2010). Poplar *RAP2.1* Potri.014G025200 and the other poplar DREB TF having Arabidopsis
401 *RAP2.1* as the closest match were significantly up-regulated in xylem both during PS and CS.
402 Consistently, the *COR413* gene Potri.007G033801 was significantly down-regulated under
403 these conditions.

404 A relationship between two (TEOSINTE BRANCHED 1, CYCLODEA, PROLIFERATING
405 CELL FACTORS (TCP) family TFs was inferred in young and mature leaves (Fig. 7B, Table
406 S8). Both TFs, Potri.013G119400 and Potri.019G091300, are most similar to the Arabidopsis
407 TF TCP4. Gene expression of Potri.013G119400 was significantly down-regulated after
408 recovery from PS both in young and mature leaves compared with untreated controls. During
409 PS and CS, both TFs were transcriptionally down-regulated in young and mature leaves
410 (Table S1). In the remaining tissues, the expression patterns of the two TFs diverged from
411 each other. For the developing xylem, Potri.013G119400 was down-regulated but
412 Potri.019G091300 was up-regulated. The putative leaf target, Potri.010G230366, does not
413 have a known function, but expression was also strongly up-regulated in the developing
414 xylem for PS and CS, and more than 50-fold after recovery from PS. Potri.013G119400 gene
415 expression was also down-regulated in phloem and roots, whereas there was no change for
416 Potri.019G091300. TCP4 has been associated with cell elongation in hypocotyls and leaf
417 morphogenesis (Challa et al., 2016). The differential regulation across tissues during stress
418 and recovery in Gray poplar may reflect different cell growth dynamics. While water deficiency

419 generally suppresses growth in above-ground poplar tissues, xylem structure and secondary
420 cell wall formation play a central role in avoiding drought damage and are highly regulated
421 (Paul et al., 2018; Sun et al., 2017).

422

423 **Common and tissue-specific processes in stress-related memory**

424 To further elucidate and compare stress-related memory processes taking place in individual
425 poplar tissues, we investigated the regulatory networks for mature leaves and developing
426 xylem (Fig. 8). These were the two tissues where the HB7 TFs, the top correlated genes
427 within and across tissues (Fig. 7B, Fig. 6A), showed the strongest post-recovery memory
428 response (Table S1). For each tissue network, we specifically focused on TFs that were
429 computationally associated with more than one putative target as predictor of gene
430 expression (Fig. 8A). Among the targets that were included in the core networks of both
431 mature leaves and developing xylem, we found two *PP2Cs* (the *HAI1* ortholog
432 (Potri.009G037300) and an *HAI3*-related *PP2C*, Potri.001G092100), the two *LATE*
433 *EMBRYOGENESIS ABUNDANT PROTEIN 4-5 (LEA 4-5)* co-orthologs and a gene of
434 unknown function with an almost 100-fold up-regulation in PS and a more than 150-fold up-
435 regulation after PS recovery in mature leaves (Potri.004G044300), whose closest Arabidopsis
436 match has been reported to be induced by ABA in guard cells (Leonhardt et al., 2004). Also
437 the two *PP2Cs* and the *LEA 4-5* co-orthologs were up-regulated both in PS and after PS
438 recovery for mature leaves (Fig. 8A). Poplar *LEA4-5* protein levels have been observed to be
439 highly increased for osmoprotection in drought stress conditions (Abraham et al., 2018). In
440 Arabidopsis, *LEA4-5* transcript and protein levels showed the largest response to ABA and
441 salt stress within the *LEA4* group (Olvera-Carrillo et al., 2010).

442 *PP2Cs* act as negative regulators of ABA signaling and hamper stomatal closure, as
443 demonstrated for example by protein interactions of the *PP2C HYPERSENSITIVE TO ABA 1*
444 (*HAB1*) in *Populus euphratica* and the *PP2C ABA-INSENSITIVE 1 (ABI1)* in *Populus*
445 *trichocarpa* as well as transgenic overexpression in Arabidopsis (Chen et al., 2015; Yu et al.,
446 2016). In Arabidopsis, the *PP2C HAI1 (SAG113; AT5G59220)* prevents stomatal closure
447 during leaf senescence and its promoter is directly targeted by a NAC TF (*NAC029, AtNAP;*
448 *AT1G69490*) (Zhang and Gan, 2012). In the mature leaf regulatory network inferred from our
449 data, expression of the *HAI1* ortholog (Potri.009G037300) was not only associated with

450 expression of the *HB7* TFs (Potri.014G103000, Potri.001G083700) but also with expression
451 of the NAC TF Potri.011G123300 and the MYB family TFs Potri.010G193000 and
452 Potri.003G100100, which belong to different ortholog groups (Fig. 8A). The association
453 between the latter three genes and the *HAI1* ortholog was not detected in developing xylem.
454 In fact, the Pearson correlation coefficients in developing xylem were 0.61, 0.30 and 0.26,
455 respectively, in contrast to the highly significant values in mature leaves (0.94, 0.91 and 0.93).
456 The gene Potri.011G123300 belongs to the NAC TF family due to its NAM (no apical
457 meristem) domain; it is a member of the NAC019-related subfamily of orthologs,
458 PTHR31719:SF82 (Mi et al., 2017). NAC TFs, and in particular the three Arabidopsis
459 members of that subfamily, NAC019, NAC055 and NAC072, are known to be of central
460 importance in drought signal transduction via the ABA-dependent pathway (Singh and Laxmi,
461 2015; Tran et al., 2004). Gene expression of the MYB TF Potri.010G193000 is negatively
462 correlated with the wood saccharification potential in poplar, which decreases with drought
463 (Wildhagen et al., 2018). Consistent with this observation, our expression data showed an up-
464 regulation of Potri.010G193000 gene expression under stress. The same pattern was
465 observed for mature leaves and in the case of PS even persisted after recovery. Furthermore,
466 Potri.010G193000 is in general co-expressed with Potri.007G085700, the TF gene *TGACG*
467 *SEQUENCE-SPECIFIC BINDING PROTEIN 1 (TGA1)* (Wildhagen et al., 2018). Interestingly,
468 several Arabidopsis orthologs of inferred regulators of *HAI1* in mature poplar leaves were
469 connected via experimental and literature-curated protein-protein interaction data
470 (Arabidopsis Interactome Mapping Consortium, 2011; Berardini et al., 2015; Yazaki et al.,
471 2016), including *TGA1* (Fig. 8B). The *TCP4* orthologs discussed above (Potri.019G091300,
472 Potri.013G119400) were strongly transcriptionally anti-correlated with the *HB7* co-ortholog
473 Potri.001G083700, which was found as a central predictor for the two *PP2Cs* and both *LEA4-*
474 *5* orthologs in mature leaves.

475 In developing xylem, the *HB7* co-ortholog Potri.001G083700 was also associated with these
476 *PP2Cs* and *LEA4-5* orthologs, which have known physiological functions related to drought.
477 In both tissues, Potri.001G083700 gene expression continued to be up-regulated after PS
478 recovery. In addition, the core networks of xylem and mature leaves shared the putative
479 target *GLUTAREDOXIN C1 (GRXC1) co-ortholog 2(of2)* (Potri.012G082800), showing post-
480 recovery PS up-regulation in both tissues. With respect to abiotic stress, *GRXC1* has roles in
481 signaling and oxidative stress tolerance (Li, 2014). Another shared putative target was

482 Potri.002G117800, one of two *NADH DEHYDROGENASE (UBIQUINONE) FE-S PROTEIN 4*
483 (*NDUFS4*) genes that are involved in the mitochondrial electron transfer chain and have been
484 associated with thermotolerance in Arabidopsis (Kim et al., 2012). With respect to additional
485 TFs, the xylem network showed several differences to the network from mature leaves (Fig.
486 8A). The ERF/AP2 DREB TF Potri.006G138900 (see also previous section) was a large hub
487 in addition to the HB7 TF Potri.001G083700, which formed a central hub in both tissues. The
488 BHLH18-related TF Potri.009G081400 (BASIC HELIX-LOOP-HELIX 18) was unique to the
489 xylem network, associated with *GRX1*, *LEA4-5* and both *PP2Cs* and still significantly up-
490 regulated after PS recovery. A xylem-specific putative regulator of both HB7 TFs was the
491 BHLH TF Potri.014G111400, one of three *PHYTOCHROME-INTERACTING FACTOR 3*
492 (*PIF3*) genes. Arabidopsis PIF3 promotes hypocotyl elongation (Soy et al., 2012; Zhong et al.,
493 2012). In summary, our data suggest that common TFs such as HB7, in particular the central
494 hub gene Potri.001G083700, work together with tissue-specific TFs to coordinate stress and
495 post-recovery processes in different tissues.

496

497 **DISCUSSION**

498 Although drought stress is one of the major threats to plant growth, it is well-known that plants
499 having endured stress can show better photosynthetic performance than non-exposed plants
500 both under subsequent stress (Wang et al., 2014) and under well-watered conditions
501 (Hagedorn et al., 2016), which may even lead to over-compensating plant growth (Xu et al.,
502 2010). We investigated Gray poplar trees that had experienced three weeks of drought-heat
503 stress. After one week of recovery, we observed not only a complete reconstitution of
504 transpiration and photosynthetic capacity along with a relaxation of water potentials but also
505 an increased rate of carbon gain compared to non-stressed controls, both for a periodic and a
506 chronic stress scenario. Transcriptomic analyses across five different organs and tissues
507 revealed cellular processes occurring in response to combined drought and heat stress and
508 after recovery. Post-recovery expression patterns showed significant differences to non-
509 treated poplar trees and also between the two stress scenarios, although the PS and CS
510 responses had been highly similar at the end of the stress phase. This observation
511 substantiates the hypothesis that stress exposure influences the physiological state of a plant
512 even after recovery and that this long-term response varies according to the frequency or

513 duration of stress intervals. This memory phenomenon of trees occurring already a few days
514 after the stress ceased hints at powerful molecular mechanisms, which potentially could also
515 make a difference in plant fitness across multiple successive years. Such a life-cycle
516 investigation was outside the scope of the current study. However, the results show that such
517 a long-term investigation might be highly valuable when carefully designed.

518 Similar expression patterns in response to stress and after recovery were found throughout
519 the tree. However, they were implemented by distinct genes in each tissue. Only a small
520 number of genes showed a consistent response profile across all tissues. Apart from genes
521 encoding signaling components and enzymes like PP2Cs and GRXC1 or proteins with
522 structural function like the LEA4-5 hydrophilins (Battaglia et al., 2008), this set of genes with
523 putatively ubiquitous function contained several TFs, most prominently two HB7 TFs that also
524 showed a PS-related post-recovery up-regulation. HB7 contains a homeodomain and a
525 leucine zipper motif. This protein architecture indicates that the TF forms dimers (Ariel et al.,
526 2007). TF homo- or heterodimerization as well as multimerization allow for a high degree of
527 regulatory fine-tuning in gene expression. We therefore speculate that TF complexes might
528 play a role in shaping stress and post-recovery regulation of gene expression in the tissue-
529 specific context (Fig. 8B). Protein-protein interaction data from the model system *Arabidopsis*
530 *thaliana* suggest that HB7 and some TFs from the NAC019 and MYB TF families with leaf-
531 specific responses in poplar (best *Arabidopsis* matches AT4G27410 and AT5G05790,
532 respectively) may all associate with TGA1 and a set of ZHD (zinc-finger homeodomain) TFs,
533 which were expressed in all poplar tissues according to our dataset. Another putative
534 interactor of TGA1, the only HEAT STRESS TRANSCRIPTION FACTOR C-1 (HSFC1) TF in
535 poplar (Potri.T137400), was predicted as a regulator of the *HB7* co-ortholog
536 Potri.001G083700 and the two *PP2Cs* in phloem-bark (Table S8). The family of ZHD TFs has
537 been shown to act as heterodimers playing a crucial role in floral development (Tan and Irish,
538 2006) as well as ABA response (Wang et al., 2011) in *Arabidopsis*. Co-expression of the
539 NAC019 family gene AT4G27410 and ZHD11 strongly induces the expression of *EARLY*
540 *RESPONSIVE TO DEHYDRATION STRESS 1*, which is up-regulated by drought through the
541 ABA-independent pathway (Tran et al., 2007).

542 Combined action of several TFs putatively regulates the expression of target genes. The up-
543 regulation of *PP2Cs* in mature poplar leaves observed in our study is consistent with the
544 positive regulatory role of HB7 in *PP2C* expression reported for *Arabidopsis* (Valdés et al.,

545 2012). Furthermore, NAC TFs regulate the *PP2C HAI1* (Zhang and Gan, 2012) and other
546 drought tolerance genes (Singh and Laxmi, 2015; Tran et al., 2004). PP2Cs inactivate SNF1-
547 related protein kinases of type 2 (SnRK2s) that are positive regulators of ABA signaling,
548 stomatal closure and chlorophyll degradation (Fujii et al., 2011; Gao et al., 2016; Kulik et al.,
549 2011; Nakashima et al., 2009; Valdés et al., 2012). Consistently, HB7 overexpression leads to
550 an increased chlorophyll content and a higher photosynthesis rate (Re et al., 2014).
551 Moreover, different PP2Cs interact with the photosynthetic machinery (Fuchs et al., 2013;
552 Samol et al., 2012), and photosynthesis genes are up-regulated in *snrk2* triple mutants
553 (Nakashima et al., 2009), proposing a relationship between PP2Cs and photosynthesis.
554 Translating these findings to poplar, the model would explain an improved photosynthesis of
555 recovered poplar trees after periodic stress (Fig. 8C). Chlorophyll content estimates did not
556 show differences to the controls (Vanzo et al., 2015) but were done non-invasively in contrast
557 to the Arabidopsis studies (Gao et al., 2016; Re et al., 2014). The increase of ABA levels
558 during drought stress inhibits enzyme activity of clade A PP2Cs like HAI1 and HAI3 via
559 interacting ABA receptors (Dupeux et al., 2011; Tischer et al., 2017). Due to this mechanism,
560 leaf stomata can close during drought to prevent excessive water loss (Fig. 8C). For poplar,
561 stress-induced stomatal closure was confirmed by our measurements of transpiration and
562 stomatal conductance. Protein-protein interactions of PP2Cs with a SnRK2 kinase and
563 pyrabactin resistance-like ABA receptors and their effect on leaf stomatal closure in
564 transgenic plants have been shown for several poplar species (Chen et al., 2015; Yu et al.,
565 2016), yielding evidence on the potential role of PP2Cs in poplar leaves during and after
566 stress. Apart from that, PP2Cs may also be involved in chromatin remodeling and the
567 establishment of an epigenetic memory after stress (Asensi-Fabado et al., 2017).

568 The system-wide gene expression rearrangement after stress recovery might also contribute
569 to the improved tolerance against future stresses described previously (Crisp et al., 2016;
570 Hilker et al., 2016; Wang et al., 2014). In Arabidopsis, HB7 and LEA4-5, prominent memory-
571 related genes from our study, are more strongly induced at repeated dehydration stress
572 challenges than at the first stress challenge (Ding et al., 2013). Complementing such studies
573 on recurrence-dependent changes in stress responses, our data provide a comprehensive
574 view on stress-related molecular memory under non-stress, post-recovery conditions. The
575 increased base levels of HB7 and LEA4-5 gene expression after stress recovery could
576 potentially explain the higher levels at subsequent stress challenges. Consistent with such a

577 model, the periodic stress response was greater than the chronic stress response in leaves
578 and the post-recovery base level increase was only significant for periodic stress and not for
579 chronic stress, suggesting a gradual base level increase along with several stress
580 experiences. The same trend was observed in the photosynthesis data. A better
581 understanding of the molecular changes, their timing and their impact on the performance of
582 plants is instrumental in providing guidelines for resource-efficient agroforestry water
583 management and in breeding of crop and tree cultivars that are genetically equipped for
584 climate change scenarios. The present evaluation indicates that transcription factors as
585 central switches of a molecular memory may be important mediators of plant fitness in
586 persistent adaptation to recurrent abiotic stress. The biological hypotheses generated by our
587 comprehensive data acquisition and integration pave the way for detailed mechanistic studies
588 that will provide deeper insights into memory-related molecular processes in plants.

589

590 **MATERIALS AND METHODS**

591

592 **Plant material**

593 The experiments were performed with wild-type plants of Gray poplar (*Populus x canescens*
594 [INRA clone 7171-B4]; syn. *Populus tremula x Populus alba*). Plantlets were amplified by
595 micro-propagation under sterile conditions (Leple et al., 1992) and raised for five weeks in
596 2.2-L pots on a sandy soil (1:1 [v/v] silica sand and Fruhstorfer Einheitserde, initially mixed
597 with slow-release fertilizers: Triabon [Compo] and Osmocote [Scotts Miracle-Gro], 1:1, 10 g L⁻¹
598 soil; every two weeks fertilized with 0.1% [w/v] Hakaphos Grün [Compo]) in the greenhouse
599 (16/8 h photoperiodicity with supplemental lighting, 200-240 μmol photons m⁻² s⁻¹ at the
600 canopy level, photosynthetically active radiation [PAR]; day/ night temperature 22 °C/ 18 °C;
601 and an ambient mean CO₂ concentration of 380 μL L⁻¹). Then the plants were moved to
602 phytotron chambers to simulate specific climate scenarios. Within each chamber, 12 plants
603 were cultivated together in a gas-tight sub-chamber made of acrylic glass (about 1 m³), which
604 enabled online analysis of canopy gas exchange (Vanzo et al., 2015).

605

606 **Simulated climate conditions and harvesting schedule**

607 The future climate scenarios simulated in our experiments comprised elevated CO₂ (EC) and
608 two abiotic stress scenarios under elevated CO₂, periodic drought-heat stress (PS) and
609 chronic drought-heat stress (CS). Before starting the abiotic stress scenarios, plants were
610 cultivated for 25 days in the phytotron chambers at control conditions (daily maximum air
611 temperature of 27°C, 50% relative air humidity) with either ambient (380 μL L⁻¹) or elevated
612 (500 μL L⁻¹) CO₂. The CO₂ concentrations in all scenarios followed natural occurring diurnal
613 variations. The elevated CO₂ environment in the EC, PS and CS scenarios was created by
614 injection of pure CO₂ (+ 120 μL L⁻¹) into the air stream of the ambient CO₂. In the chronic
615 stress treatment, irrigation was gradually reduced for 22 days, down to 70% reduction
616 compared with the controls. The periodic stress treatment included three cycles of reduced
617 irrigation (50%, 60% and 70% reduction compared to controls), each one lasting for six days;
618 between the cycles, there were recovery periods lasting two days. In both stress scenarios,
619 the daily maximum air temperature was set to 33°C during periods with reduced irrigation.
620 Non-invasive gas exchange measurements were made continuously; destructive harvests of
621 six plants per chamber were performed at the end of the stress phase and after one week of
622 recovery (Vanzo et al., 2015). Mid-day shoot water potentials (ψ_{md}) were determined at each
623 sampling date (n=6 plants per treatment, mean \pm se) using a Scholander pressure chamber
624 (Scholander et al., 1965). In chronically and periodically stress-treated plants ψ_{md} was more
625 negative (-1.52 \pm 0.10 and -1.27 \pm 0.05 MPa, respectively) compared to a ψ_{md} of -0.97 \pm 0.04
626 MPa in AC and of -0.97 \pm 0.07 MPa in EC shoots. At recovery ψ_{md} went back to -0.72 \pm 0.10
627 and -0.93 \pm 0.07 MPa in PS and CS, respectively, reaching comparable values as the
628 untreated controls in AC (-0.77 \pm 0.07 MPa) and EC (-0.90 \pm 0.06 MPa).

629

630 **Gas exchange measurements**

631 Leaf-level gas exchange measurements were performed using two GFS-3000 instruments
632 (Walz, Germany) with an 8 cm² clip-on-type cuvette on attached leaves (no. 9 from the apex)
633 of four biological replicates under standard conditions (30°C, 1000 μmol photons m⁻² s⁻¹, and
634 air humidity of 10,000 μL L⁻¹). The cuvette was flushed with synthetic air having the CO₂
635 concentration of the respective growth condition. For each climate chamber, CO₂ and water
636 concentrations in the ambient air were measured every 20 min with two infrared gas

637 analyzers (Rosemount 100/4P, Walz, Germany) from the outlet of the gas-tight sub-chamber
638 with the plants. Inlet air was also measured every 20 min. From the difference between the
639 outlet and inlet concentrations of each sub-chamber, the whole plant (canopy) net CO₂
640 exchange and evapotranspiration were calculated according to the equation of von
641 Caemmerer and Farquhar (von Caemmerer and Farquhar, 1981). These fluxes of CO₂ and
642 water were then normalized using the canopy leaf area estimation of every given day (Jud et
643 al., 2016; Vanzo et al., 2015).

644

645 **Organ and tissue sampling**

646 Plants were harvested at noon at the last day of stress treatment and seven days later at the
647 end of the recovery period. Leaves (young leaves n. 4-6, mature leaves n. 9-12 counting from
648 the apex, respectively) were immediately frozen in liquid N₂. A stem segment of 10 cm was
649 cut 10 cm above the stem base and immediately frozen in liquid N₂. The roots were washed
650 three times in water, carefully dabbed with filter paper and then also frozen in liquid N₂. All
651 material was stored at -80 °C until homogenization. Homogenization of plant materials was
652 performed under liquid N₂ with mortar and pestle. The bark containing the phloem tissue was
653 removed from the stem section with a scalpel. Young developing xylem tissue was obtained
654 by scraping off the first 1-2 mm of the hardwood section. The homogenized material of mature
655 leaves was used both for biochemical analysis and RNA extraction, all other material only for
656 RNA extraction. Although leaf and root samples are mixtures of several tissues, the different
657 plant materials are referred to as tissues throughout this work.

658

659 **Biochemical measurements of the antioxidative system**

660 Enzyme activities and molecular antioxidant levels from four biological replicates were
661 determined as previously described (AbdElgawad et al., 2016). Molecular antioxidants were
662 quantified by HPLC, after extraction of frozen plant material in hexane (tocopherols) or in ice-
663 cold meta-phosphoric acid (ascorbate, glutathione). Enzyme activities for superoxide
664 dismutase, peroxidase, catalase, ascorbate peroxidase, glutathione peroxidase, glutathione
665 reductase, dehydroascorbate reductase, and monodehydroascorbate reductase were

666 determined using a micro-plate reader after extraction of frozen plant material in potassium
667 phosphate buffer supplemented with protease inhibitors.

668

669 **RNA-seq analysis**

670 RNA extraction was performed as described by Bi et al. (Bi et al., 2015). Total RNA was
671 extracted from 50 mg frozen tissue using the Aurum Total RNA Mini kit (Bio-Rad, Germany)
672 following the manufacturer's instructions. The RNA concentration was quantified using a
673 NanoDrop 1000 photometer (NanoDrop, Peqlab GmbH, Erlangen, Germany). The 260/230
674 and 260/280 ratios were in the range of 1.90 to 2.67 (mean 2.21) and 1.94 to 2.45 (mean
675 2.12), respectively. RNA integrity was confirmed by an Agilent Bioanalyzer 2100 (Agilent
676 Technologies, USA). For each specific combination of environmental condition, time point and
677 tissue, RNA samples from three biological replicates were analyzed by Illumina sequencing
678 (100 bp single reads, HiSeq 2500, Illumina, Inc., San Diego, CA, USA) of mRNA libraries
679 (NEBNext Ultra directional RNA library prep Kit Illumina, New England Biolabs, Inc., Ipswich,
680 MA, USA), yielding RNA-seq reads for 120 samples in total. The biological replicates are
681 samples from different individual trees grown under the same condition and harvested at the
682 same time. For each tree, samples from all five tissues were sequenced, except for two cases
683 where RNA extraction from the initial sample failed (260/230 ratio 0.42 and 1.4, respectively)
684 and samples from additional trees had to be taken as replacement: AC recovery root sample
685 replicate 1 and PS stress xylem sample replicate 3 (Table S9). RNA-seq reads were aligned
686 against the repeat-masked version of the *Populus trichocarpa* reference genome (assembly
687 version v3.0) (Tuskan et al., 2006) using TopHat2 (Kim et al., 2013). To account for the
688 evolutionary distance between Gray poplar and the used reference genome, different
689 alignment stringency levels were tested. For that purpose, three different sequencing libraries
690 were randomly selected and RNA-seq reads mapped against the reference genome allowing
691 from two up to six mapping errors per read (Fig. S2). About 70% of the RNA-seq reads were
692 aligned when allowing a maximum of five errors in the read alignments, which is relatively
693 similar to RNA-seq analysis in other plants (International Barley Genome Sequencing
694 Consortium et al., 2012). Due to the relatively constant proportion of uniquely mapped reads
695 for the considered error levels (Fig. S2B), we continued the analysis with the maximum
696 threshold of five errors (Fig. S3).

697 Based on the read alignments and the *P. trichocarpa* annotation version v3.1 at the
698 Phytozome platform (Goodstein et al., 2012; Tuskan et al., 2006), TPM gene expression
699 levels were calculated using StringTie version 1.3.4 (Pertea et al., 2015). The biological
700 replicates showed high Pearson correlation coefficients (computed by the cor function in R
701 version 3.5.0 (R Core Team, 2018)) except for one single case (Fig. S4), which was excluded
702 from further analysis. Differentially expressed genes between PS or CS and EC groups were
703 identified by the R package DESeq2 version 1.20.0 (Love et al., 2014) using the script
704 provided at <http://ccb.jhu.edu/software/stringtie/dl/prepDE.py>. Gene annotation including
705 functional description and Gene Ontology (GO) terms were retrieved from the *Populus*
706 *trichocarpa* reference annotation version v3.1 at the Phytozome platform (Goodstein et al.,
707 2012; Tuskan et al., 2006). GO enrichment analysis for categories with at least fifty genes
708 was performed in R version 3.5.0 (R Core Team, 2018) using fisher.test and multiple testing
709 correction by p.adjust using the false discovery rate (FDR) method.

710

711 **Co-expression network analysis**

712 The co-expression network analysis focused on the environmental conditions with elevated
713 CO₂ levels, omitting the AC (ambient CO₂) condition. For each tissue, log₂(TPM+1)-
714 transformed gene expression levels were averaged for each condition and time point and
715 genes were filtered for a minimum coefficient of variation of 0.3 (Fig. S5). Individual co-
716 expression modules for each tissue were determined using the R packages WGCNA version
717 1.64-1, flashClust version 1.01-2 and dynamicTreeCut version 1.63-1 (Langfelder and
718 Horvath, 2008, 2012; Langfelder et al., 2008). The parameters were set to "hybrid signed"
719 network, "average" agglomeration, split sensitivity 1 and a minimum cluster size of 50. Then
720 the module eigengenes (Langfelder and Horvath, 2007), characteristic expression profiles of
721 modules, were clustered across all tissues into communities, according to their correlation.
722 This step was performed using again flashClust and dynamicTreeCut ("average"
723 agglomeration, deep split set to true and a minimum cluster size of 2). Communities that
724 contain modules from all five tissues were visualized with the tkplot and plot functions in the R
725 package igraph version 1.2.2 (Csardi and Nepusz, 2006). The corresponding heatmaps were
726 plotted using the R packages pheatmap version 1.0.10, gridExtra version 2.3 and ggplot2
727 version 2.2.1 (Auguie, 2017; Kolde, 2018; Wickham, 2009).

728

729 **Between-tissue correlations and gene regulatory network analysis**

730 To investigate tissue-specific regulation of universally responding genes, we first determined
731 individual genes that behaved similarly in all the tissues and then predicted their regulation by
732 transcription factors (TFs) using the RNA-seq data. In the first step, gene-gene correlations
733 across individual trees from all treatment groups were computed using the `cor` function in R
734 version 3.5.0 on the $\log_2(\text{TPM}+1)$ -transformed gene expression data (R Core Team, 2018). In
735 particular, correlation values of the same gene across all pairs of tissues were recorded and
736 the 17 genes with a median greater than 0.8 and significant post-recovery difference to
737 controls in at least one tissue ($\text{abs}(\log_2 \text{ fold change}) > 1$ and $p.\text{adj} < 0.05$ according to the
738 DESeq2 analysis) were selected as query genes for further analysis. Since observations for
739 these genes were quite complete (less than twenty values with expression level zero in the
740 whole dataset with 119 samples), we focused the regulatory network analysis on genes with
741 at most twenty zero values. TF family annotation for *Populus trichocarpa* and *Arabidopsis*
742 *thaliana* was downloaded from PlantTFDB (Jin et al., 2014) on 03.09.2018. Poplar genes
743 were included as candidate TFs in the analysis if they themselves as well as their best
744 Arabidopsis match according to the Phytozome annotation v3.1 (Goodstein et al., 2012;
745 Tuskan et al., 2006) were both classified as TFs, resulting in 1346 candidates. For each query
746 gene, the top regulatory candidates were determined from the gene expression data of each
747 tissue separately using the R package GENIE3 version 1.2.1 (Aibar et al., 2017; Huynh-Thu
748 et al., 2010). Networks were drawn with the R package igraph version 1.2.2 (Csardi and
749 Nepusz, 2006). For visualization purposes, the top five candidates are shown for each query
750 gene.

751

752 **Protein-protein interaction analysis**

753 Experimental and literature-curated protein-protein interaction data for *Arabidopsis thaliana*
754 were obtained from datasets of interactome publications and from the TairProteinInteraction
755 file (time stamp: 2011-08-23) at The Arabidopsis Information Resource (Arabidopsis
756 Interactome Mapping Consortium., 2011; Berardini et al., 2015; Yazaki et al., 2016) and
757 compiled into a single network. The network was visualized with Graphviz version 2.36

758 (Gansner and North, 2000). Due to the prominent transcriptional stress-related memory
759 response observed for the HB7 TF Potri.001G083700 and its predicted target, the HAI1
760 ortholog Potri.009G037300, combined with the known physiological role of HAI1 in
761 *Arabidopsis thaliana* leaves and the dimerization motif of HB7, we investigated the
762 interactomes of Arabidopsis orthologs for all TFs that were predicted to regulate
763 Potri.009G037300 in mature leaves and showed a significant differential expression in PS vs.
764 EC after recovery. The subnetwork connecting AT2G46680 (HB7) and AT4G27410 (closest
765 match from the NAC019 orthology group) was evident from visual inspection of the network,
766 and the connection to the MYB TF AT5G05790 was found computationally by neighborhood
767 intersection. All three TFs did not have any other interactions than the ones shown in the
768 subnetwork (Fig. 8B).

769

770 **Further statistical analysis**

771 Treatment group comparisons for the gas exchange and antioxidant data were performed
772 using the R package `dunn.test` with the FDR method "bh" as a post-hoc Dunn's test after
773 application of the Kruskal-Wallis test using `kruskal.test` in R version 3.5.0 (R Core Team,
774 2018). Dimension reduction for data visualization was also done in R. To show common
775 variation between the gas exchange data (eight parameters) and the $\log_2(\text{TPM}+1)$ -
776 transformed gene expression data in mature leaves, we selected the hundred most varying
777 genes and applied regularized canonical correlation analysis using the `rcc` function from the
778 `mixOmics` package version 6.3.2 (Gonzalez et al., 2011; Le Cao et al., 2009) and an
779 analytical estimate of the regularization parameter (Schäfer and Strimmer, 2005). Principal
780 component analysis of the whole gene expression dataset was performed with the `prcomp`
781 function in R version 3.5.0 (R Core Team, 2018). Ellipses for 75% confidence levels were
782 constructed from the expression data using the `dataEllipse` function of the R package `car`
783 version 3.0-2 (Fox and Weisberg, 2011). Venn diagrams for differentially expressed genes
784 ($|\text{abs}(\log_2 \text{ fold change})| > 1$ and $p.\text{adj} < 0.05$ according to the DESeq2 analysis) were created
785 with the R package `venn` version 1.7 (Dusa, 2018), and the gene-wise expression heatmap
786 was generated with the `heatmap.2` function of the `gplots` R package version 3.0.1 (Warnes et
787 al., 2016).

788

789 **Accession numbers**

790 The RNA-seq data have been deposited in the ArrayExpress database at EMBL-EBI
791 (<https://www.ebi.ac.uk/arrayexpress/experiments/E-MTAB-6121>). R scripts for the data
792 analysis are available at <https://github.com/georgii-helmholtz/samm>.

793

794 **Supplemental Data**

795 SupplementalFigures.pdf (includes legends for Supp. Tables)

796 SuppTableS1.xlsx

797 SuppTableS2.xlsx

798 SuppTableS3.xlsx

799 SuppTableS4.xlsx

800 SuppTableS5.xlsx

801 SuppTableS6.xlsx

802 SuppTableS7.xlsx

803 SuppTableS8.xlsx

804 SuppTableS9.xlsx

805

806 **Acknowledgements**

807 The work was financially supported by the European Science Foundation (ESF) Eurocores
808 programme 'EuroVOL' within the joint research project 'MOMEVIP', the European Plant
809 Phenotyping Network (EPPN) funded by the EU FP7 Research Infrastructures Programme
810 [no. 284443], the German Ministry of Education and Research projects 'PROBIOPA' [no.
811 0315412] and German Plant Phenotyping Network (DPPN) [no. 031A053C], the Belgian Fund
812 for Scientific Research [no. GA13511N] and by the Austrian Science Funds [no. I655-B16].

813 The authors thank Pascal Falter-Braun, Daniel Lang and Georg Haberer for helpful
814 comments.

815 **Author contributions**

816 J.-P.S., K.F.X.M., K.P., H.A. and A.H. designed the research. E.V., M.A.D., W.J. and R.R.
817 performed the experiments. E.G., K.K., M.P., K.B., H.AE. and M.S. analyzed the data. E.G.
818 wrote the paper with contributions of J.-P.S., K.F.X.M., K.K., K.P., A.R.S. and M.S.; all
819 authors checked and revised the manuscript.

820

821 **REFERENCES**

822

823 AbdElgawad, H., Zinta, G., Hegab, M.M., Pandey, R., Asard, H., and Abuelsoud, W. (2016).
824 High salinity induces different oxidative stress and antioxidant responses in maize seedlings
825 organs. *Front. Plant Sci.* 7: 276.

826 Abraham, P.E., Garcia, B.J., Gunter, L.E., Jawdy, S.S., Engle, N., Yang, X., Jacobson, D.A.,
827 Hettich, R.L., Tuskan, G.A., and Tschaplinski, T.J. (2018). Quantitative proteome profile of
828 water deficit stress responses in eastern cottonwood (*Populus deltoides*) leaves. *PLoS One*
829 13: e0190019.

830 Aibar, S., Gonzalez-Blas, C.B., Moerman, T., Huynh-Thu, V.A., Imrichova, H., Hulselmans,
831 G., Rambow, F., Marine, J.C., Geurts, P., Aerts, J., et al. (2017). SCENIC: single-cell
832 regulatory network inference and clustering. *Nat. Methods* 14: 1083-1086.

833 Arabidopsis Interactome Mapping Consortium (2011). Evidence for network evolution in an
834 Arabidopsis interactome map. *Science* 333: 601-607.

835 Ariel, F.D., Manavella, P.A., Dezar, C.A., and Chan, R.L. (2007). The true story of the HD-Zip
836 family. *Trends Plant Sci.* 12: 419-426.

837 Aroca, R., Porcel, R., and Ruiz-Lozano, J.M. (2012). Regulation of root water uptake under
838 abiotic stress conditions. *J. Exp. Bot.* 63: 43-57.

839 Asensi-Fabado, M.A., Amtmann, A., and Perrella, G. (2017). Plant responses to abiotic
840 stress: The chromatin context of transcriptional regulation. *Biochim. Biophys. Acta* 1860: 106-
841 122.

842 Auguie, B. (2017). gridExtra: Miscellaneous Functions for "Grid" Graphics.

843 Battaglia, M., Olvera-Carrillo, Y., Garcarrubio, A., Campos, F., and Covarrubias, A.A. (2008).
844 The enigmatic LEA proteins and other hydrophilins. *Plant Physiol.* 148: 6-24.

845 Berardini, T.Z., Reiser, L., Li, D., Mezheritsky, Y., Muller, R., Strait, E., and Huala, E. (2015).
846 The Arabidopsis information resource: Making and mining the "gold standard" annotated
847 reference plant genome. *Genesis* 53: 474-485.

848 Bi, Z., Merl-Pham, J., Uehlein, N., Zimmer, I., Mühlhans, S., Aichler, M., Walch, A.K.,
849 Kaldenhoff, R., Palme, K., Schnitzler, J.P., et al. (2015). RNAi-mediated downregulation of
850 poplar plasma membrane intrinsic proteins (PIPs) changes plasma membrane proteome
851 composition and affects leaf physiology. *J. Proteomics* 128: 321-332.

852 Bloemen, J., Vergeynst, L.L., Overlaet-Michiels, L., and Steppe, K. (2016). How important is
853 woody tissue photosynthesis in poplar during drought stress? *Trees* 30: 63-72.

854 Challa, K.R., Aggarwal, P., and Nath, U. (2016). Activation of YUCCA5 by the Transcription
855 Factor TCP4 Integrates Developmental and Environmental Signals to Promote Hypocotyl
856 Elongation in Arabidopsis. *Plant Cell*.

857 Chen, J., Zhang, D., Zhang, C., Xia, X., Yin, W., and Tian, Q. (2015). A Putative PP2C-
858 Encoding Gene Negatively Regulates ABA Signaling in *Populus euphratica*. *PLoS One* 10:
859 e0139466.

860 Crisp, P.A., Ganguly, D., Eichten, S.R., Borevitz, J.O., and Pogson, B.J. (2016).
861 Reconsidering plant memory: Intersections between stress recovery, RNA turnover, and
862 epigenetics. *Sci. Adv.* 2: e1501340.

863 Csardi, G., and Nepusz, T. (2006). The igraph software package for complex network
864 research. *InterJournal Complex Systems*: 1695.

865 Ding, Y., Fromm, M., and Avramova, Z. (2012). Multiple exposures to drought 'train'
866 transcriptional responses in Arabidopsis. *Nat Commun* 3: 740.

867 Ding, Y., Liu, N., Virilouvet, L., Riethoven, J.J., Fromm, M., and Avramova, Z. (2013). Four
868 distinct types of dehydration stress memory genes in Arabidopsis thaliana. *BMC Plant Biol.*
869 13: 229.

870 Dong, C.J., and Liu, J.Y. (2010). The Arabidopsis EAR-motif-containing protein RAP2.1
871 functions as an active transcriptional repressor to keep stress responses under tight control.
872 *BMC Plant Biol.* 10: 47.

873 Dupeux, F., Antoni, R., Betz, K., Santiago, J., Gonzalez-Guzman, M., Rodriguez, L., Rubio,
874 S., Park, S.Y., Cutler, S.R., Rodriguez, P.L., et al. (2011). Modulation of abscisic acid

875 signaling in vivo by an engineered receptor-insensitive protein phosphatase type 2C allele.
876 *Plant Physiol.* 156: 106-116.

877 Dusa, A. (2018). venn: Draw Venn Diagrams.

878 Fleta-Soriano, E., and Munne-Bosch, S. (2016). Stress Memory and the Inevitable Effects of
879 Drought: A Physiological Perspective. *Front. Plant Sci.* 7: 143.

880 Fox, J., and Weisberg, S. (2011). *An R Companion to Applied Regression* (Sage).

881 Fuchs, S., Grill, E., Meskiene, I., and Schweighofer, A. (2013). Type 2C protein phosphatases
882 in plants. *FEBS J.* 280: 681-693.

883 Fujii, H., Verslues, P.E., and Zhu, J.K. (2011). *Arabidopsis* decuple mutant reveals the
884 importance of SnRK2 kinases in osmotic stress responses in vivo. *Proc Natl Acad Sci U S A*
885 108: 1717-1722.

886 Gansner, E.R., and North, S.C. (2000). An open graph visualization system and its
887 applications to software engineering. *SOFTWARE - PRACTICE AND EXPERIENCE* 30:
888 1203-1233.

889 Gao, S., Gao, J., Zhu, X., Song, Y., Li, Z., Ren, G., Zhou, X., and Kuai, B. (2016). ABF2,
890 ABF3, and ABF4 Promote ABA-Mediated Chlorophyll Degradation and Leaf Senescence by
891 Transcriptional Activation of Chlorophyll Catabolic Genes and Senescence-Associated Genes
892 in *Arabidopsis*. *Mol Plant* 9: 1272-1285.

893 Gonzalez, I., Le Cao, K.A., and Dejean, S. (2011). mixOmics: Omics data integration project.

894 Goodstein, D.M., Shu, S., Howson, R., Neupane, R., Hayes, R.D., Fazo, J., Mitros, T., Dirks,
895 W., Hellsten, U., Putnam, N., et al. (2012). Phytozome: a comparative platform for green plant
896 genomics. *Nucleic Acids Res.* 40: D1178-1186.

897 Hagedorn, F., Joseph, J., Peter, M., Luster, J., Pritsch, K., Geppert, U., Kerner, R., Molinier,
898 V., Egli, S., Schaub, M., et al. (2016). Recovery of trees from drought depends on
899 belowground sink control. *Nat. Plants* 2: 16111.

900 Harfouche, A., Meilan, R., and Altman, A. (2014). Molecular and physiological responses to
901 abiotic stress in forest trees and their relevance to tree improvement. *Tree Physiol* 34: 1181-
902 1198.

903 Hilker, M., Schwachtje, J., Baier, M., Balazadeh, S., Baurle, I., Geiselhardt, S., Hinch, D.K.,
904 Kunze, R., Mueller-Roeber, B., Rillig, M.C., et al. (2016). Priming and memory of stress
905 responses in organisms lacking a nervous system. *Biol. Rev. Camb. Philos. Soc.* 91: 1118-
906 1133.

907 Hjellström, M., Olsson, A.S.B., Engström, O., and Söderman, E.M. (2003). Constitutive
908 expression of the water deficit-inducible homeobox gene *ATHB7* in transgenic *Arabidopsis*
909 causes a suppression of stem elongation growth. *Plant Cell Environ.* 26: 1127-1136.

910 Huynh-Thu, V.A., Irrthum, A., Wehenkel, L., and Geurts, P. (2010). Inferring regulatory
911 networks from expression data using tree-based methods. *PLoS One* 5.

912 International Barley Genome Sequencing Consortium, Mayer, K.F., Waugh, R., Brown, J.W.,
913 Schulman, A., Langridge, P., Platzer, M., Fincher, G.B., Muehlbauer, G.J., Sato, K., et al.
914 (2012). A physical, genetic and functional sequence assembly of the barley genome. *Nature*
915 491: 711-716.

916 IPCC (2014). Near-term Climate Change: Projections and Predictability. In *Climate Change*
917 2013: The Physical Science Basis. Contribution of Working Group I to the Fifth Assessment
918 Report of the Intergovernmental Panel on Climate Change, T.F. Stocker, D. Qin, G.K.
919 Plattner, M. Tignor, S.K. Allen, J. Boschung, A. Nauels, Y. Xia, B. V., and P.M. Midgley, eds.
920 (Cambridge: Cambridge University Press).

921 Jin, J., Zhang, H., Kong, L., Gao, G., and Luo, J. (2014). PlantTFDB 3.0: a portal for the
922 functional and evolutionary study of plant transcription factors. *Nucleic Acids Res.* 42: D1182-
923 1187.

924 Jud, W., Vanzo, E., Li, Z., Ghirardo, A., Zimmer, I., Sharkey, T.D., Hansel, A., and Schnitzler,
925 J.P. (2016). Effects of heat and drought stress on post-illumination bursts of volatile organic
926 compounds in isoprene-emitting and non-emitting poplar. *Plant Cell Environ.* 39: 1204-1215.

927 Kim, D., Pertea, G., Trapnell, C., Pimentel, H., Kelley, R., and Salzberg, S.L. (2013).
928 TopHat2: accurate alignment of transcriptomes in the presence of insertions, deletions and
929 gene fusions. *Genome Biol.* 14: R36.

930 Kim, M., Lee, U., Small, I., des Francs-Small, C.C., and Vierling, E. (2012). Mutations in an
931 *Arabidopsis* mitochondrial transcription termination factor-related protein enhance
932 thermotolerance in the absence of the major molecular chaperone HSP101. *Plant Cell* 24:
933 3349-3365.

934 Kolde, R. (2018). pheatmap: Pretty Heatmaps.

935 Kotak, S., Larkindale, J., Lee, U., von Koskull-Doring, P., Vierling, E., and Scharf, K.D. (2007).
936 Complexity of the heat stress response in plants. *Curr. Opin. Plant Biol.* 10: 310-316.

937 Kulik, A., Wawer, I., Krzywinska, E., Bucholc, M., and Dobrowolska, G. (2011). SnRK2 protein
938 kinases--key regulators of plant response to abiotic stresses. *OMICS* 15: 859-872.

939 Lämke, J., Brzezinka, K., Altmann, S., and Bäurle, I. (2016). A hit-and-run heat shock factor
940 governs sustained histone methylation and transcriptional stress memory. *EMBO J.* 35: 162-
941 175.

942 Langfelder, P., and Horvath, S. (2007). Eigengene networks for studying the relationships
943 between co-expression modules. *BMC Syst. Biol.* 1: 54.

944 Langfelder, P., and Horvath, S. (2008). WGCNA: an R package for weighted correlation
945 network analysis. *BMC Bioinformatics* 9: 559.

946 Langfelder, P., and Horvath, S. (2012). Fast R Functions for Robust Correlations and
947 Hierarchical Clustering. *J Stat Softw* 46.

948 Langfelder, P., Zhang, B., and Horvath, S. (2008). Defining clusters from a hierarchical cluster
949 tree: the Dynamic Tree Cut package for R. *Bioinformatics* 24: 719-720.

950 Le Cao, K.A., Gonzalez, I., and Dejean, S. (2009). integrOmics: an R package to unravel
951 relationships between two omics datasets. *Bioinformatics* 25: 2855-2856.

952 Leonhardt, N., Kwak, J.M., Robert, N., Waner, D., Leonhardt, G., and Schroeder, J.I. (2004).
953 Microarray expression analyses of Arabidopsis guard cells and isolation of a recessive
954 abscisic acid hypersensitive protein phosphatase 2C mutant. *Plant Cell* 16: 596-615.

955 Leple, J.C., Brasileiro, A.C., Michel, M.F., Delmotte, F., and Jouanin, L. (1992). Transgenic
956 poplars: expression of chimeric genes using four different constructs. *Plant Cell Rep.* 11: 137-
957 141.

958 Li, S. (2014). Redox Modulation Matters: Emerging Functions for Glutaredoxins in Plant
959 Development and Stress Responses. *Plants (Basel)* 3: 559-582.

960 Lippold, F., vom Dorp, K., Abraham, M., Holzl, G., Wewer, V., Yilmaz, J.L., Lager, I.,
961 Montandon, C., Besagni, C., Kessler, F., et al. (2012). Fatty acid phytol ester synthesis in
962 chloroplasts of Arabidopsis. *Plant Cell* 24: 2001-2014.

963 Liu, N., Staswick, P.E., and Avramova, Z. (2016). Memory responses of jasmonic acid-
964 associated Arabidopsis genes to a repeated dehydration stress. *Plant Cell Environ.* 39: 2515-
965 2529.

966 Love, M.I., Huber, W., and Anders, S. (2014). Moderated estimation of fold change and
967 dispersion for RNA-seq data with DESeq2. *Genome Biol.* 15: 550.

968 Mi, H., Huang, X., Muruganujan, A., Tang, H., Mills, C., Kang, D., and Thomas, P.D. (2017).
969 PANTHER version 11: expanded annotation data from Gene Ontology and Reactome
970 pathways, and data analysis tool enhancements. *Nucleic Acids Res.* 45: D183-D189.

971 Nakashima, K., Fujita, Y., Kanamori, N., Katagiri, T., Umezawa, T., Kidokoro, S., Maruyama,
972 K., Yoshida, T., Ishiyama, K., Kobayashi, M., et al. (2009). Three Arabidopsis SnRK2 protein
973 kinases, SRK2D/SnRK2.2, SRK2E/SnRK2.6/OST1 and SRK2I/SnRK2.3, involved in ABA
974 signaling are essential for the control of seed development and dormancy. *Plant Cell Physiol.*
975 50: 1345-1363.

976 Nakashima, K., Yamaguchi-Shinozaki, K., and Shinozaki, K. (2014). The transcriptional
977 regulatory network in the drought response and its crosstalk in abiotic stress responses
978 including drought, cold, and heat. *Front. Plant Sci.* 5: 170.

979 Olvera-Carrillo, Y., Campos, F., Reyes, J.L., Garcarrubio, A., and Covarrubias, A.A. (2010).
980 Functional analysis of the group 4 late embryogenesis abundant proteins reveals their
981 relevance in the adaptive response during water deficit in Arabidopsis. *Plant Physiol.* 154:
982 373-390.

983 Osakabe, Y., Osakabe, K., Shinozaki, K., and Tran, L.S. (2014). Response of plants to water
984 stress. *Front. Plant Sci.* 5: 86.

985 Paul, S., Wildhagen, H., Janz, D., and Polle, A. (2018). Drought effects on the tissue- and
986 cell-specific cytokinin activity in poplar. *AoB Plants* 10: plx067.

987 Perteua, M., Perteua, G.M., Antonescu, C.M., Chang, T.C., Mendell, J.T., and Salzberg, S.L.
988 (2015). StringTie enables improved reconstruction of a transcriptome from RNA-seq reads.
989 *Nat. Biotechnol.* 33: 290-295.

990 Pfanz, H., Aschan, G., Langenfeld-Heyser, R., Wittmann, C., and Loose, M. (2002). Ecology
991 and ecophysiology of tree stems: cortical and wood photosynthesis. *Naturwissenschaften*
992 89: 147-162.

993 R Core Team (2018). R: A Language and Environment for Statistical Computing.

994 Re, D.A., Capella, M., Bonaventure, G., and Chan, R.L. (2014). Arabidopsis AtHB7 and
995 AtHB12 evolved divergently to fine tune processes associated with growth and responses to
996 water stress. *BMC Plant Biol.* 14: 150.

997 Samol, I., Shapiguzov, A., Ingelsson, B., Fucile, G., Crevecoeur, M., Vener, A.V., Rochaix,
998 J.D., and Goldschmidt-Clermont, M. (2012). Identification of a photosystem II phosphatase
999 involved in light acclimation in Arabidopsis. *Plant Cell* 24: 2596-2609.

1000 Sani, E., Herzyk, P., Perrella, G., Colot, V., and Amtmann, A. (2013). Hyperosmotic priming of
1001 Arabidopsis seedlings establishes a long-term somatic memory accompanied by specific
1002 changes of the epigenome. *Genome Biol.* 14: R59.

1003 Schäfer, J., and Strimmer, K. (2005). A shrinkage approach to large-scale covariance matrix
1004 estimation and implications for functional genomics. *Stat Appl Genet Mol Biol* 4: Article32.

1005 Scholander, P.F., Bradstreet, E.D., Hemmingsen, E.A., and Hammel, H.T. (1965). Sap
1006 Pressure in Vascular Plants: Negative hydrostatic pressure can be measured in plants.
1007 *Science* 148: 339-346.

1008 Shinozaki, K., and Yamaguchi-Shinozaki, K. (2007). Gene networks involved in drought
1009 stress response and tolerance. *J. Exp. Bot.* 58: 221-227.

1010 Singh, D., and Laxmi, A. (2015). Transcriptional regulation of drought response: a tortuous
1011 network of transcriptional factors. *Front. Plant Sci.* 6: 895.

1012 Söderman, E., Mattsson, J., and Engström, P. (1996). The *Arabidopsis* homeobox gene
1013 *ATHB-7* is induced by water deficit and by abscisic acid. *Plant J.* 10: 375-381.

1014 Soy, J., Leivar, P., Gonzalez-Schain, N., Sentandreu, M., Prat, S., Quail, P.H., and Monte, E.
1015 (2012). Phytochrome-imposed oscillations in PIF3 protein abundance regulate hypocotyl
1016 growth under diurnal light/dark conditions in *Arabidopsis*. *Plant J.* 71: 390-401.

1017 Sun, X., Wang, C., Xiang, N., Li, X., Yang, S., Du, J., Yang, Y., and Yang, Y. (2017).
1018 Activation of secondary cell wall biosynthesis by miR319-targeted TCP4 transcription factor.
1019 *Plant Biotechnol. J.* 15: 1284-1294.

1020 Sundell, D., Street, N.R., Kumar, M., Mellerowicz, E.J., Kucukoglu, M., Johnsson, C., Kumar,
1021 V., Mannapperuma, C., Delhomme, N., Nilsson, O., et al. (2017). *AspWood*: High-Spatial-
1022 Resolution Transcriptome Profiles Reveal Uncharacterized Modularity of Wood Formation in
1023 *Populus tremula*. *Plant Cell* 29: 1585-1604.

1024 Tan, Q.K., and Irish, V.F. (2006). The *Arabidopsis* zinc finger-homeodomain genes encode
1025 proteins with unique biochemical properties that are coordinately expressed during floral
1026 development. *Plant Physiol.* 140: 1095-1108.

1027 Taylor, G. (2002). *Populus*: arabidopsis for forestry. Do we need a model tree? *Ann. Bot.* 90:
1028 681-689.

1029 Tischer, S.V., Wunschel, C., Papacek, M., Kleigrew, K., Hofmann, T., Christmann, A., and
1030 Grill, E. (2017). Combinatorial interaction network of abscisic acid receptors and coreceptors
1031 from *Arabidopsis thaliana*. *Proc Natl Acad Sci U S A* 114: 10280-10285.

1032 Tran, L.S., Nakashima, K., Sakuma, Y., Osakabe, Y., Qin, F., Simpson, S.D., Maruyama, K.,
1033 Fujita, Y., Shinozaki, K., and Yamaguchi-Shinozaki, K. (2007). Co-expression of the stress-
1034 inducible zinc finger homeodomain ZFHD1 and NAC transcription factors enhances
1035 expression of the ERD1 gene in *Arabidopsis*. *Plant J.* 49: 46-63.

1036 Tran, L.S., Nakashima, K., Sakuma, Y., Simpson, S.D., Fujita, Y., Maruyama, K., Fujita, M.,
1037 Seki, M., Shinozaki, K., and Yamaguchi-Shinozaki, K. (2004). Isolation and functional analysis
1038 of Arabidopsis stress-inducible NAC transcription factors that bind to a drought-responsive
1039 cis-element in the early responsive to dehydration stress 1 promoter. *Plant Cell* 16: 2481-
1040 2498.

1041 Tuskan, G.A., Difazio, S., Jansson, S., Bohlmann, J., Grigoriev, I., Hellsten, U., Putnam, N.,
1042 Ralph, S., Rombauts, S., Salamov, A., et al. (2006). The genome of black cottonwood,
1043 *Populus trichocarpa* (Torr. & Gray). *Science* 313: 1596-1604.

1044 Valdés, A.E., Overnäs, E., Johansson, H., Rada-Iglesias, A., and Engström, P. (2012). The
1045 homeodomain-leucine zipper (HD-Zip) class I transcription factors ATHB7 and ATHB12
1046 modulate abscisic acid signalling by regulating protein phosphatase 2C and abscisic acid
1047 receptor gene activities. *Plant Mol. Biol.* 80: 405-418.

1048 Vanzo, E., Jud, W., Li, Z., Albert, A., Domagalska, M.A., Ghirardo, A., Niederbacher, B.,
1049 Frenzel, J., Beemster, G.T., Asard, H., et al. (2015). Facing the Future: Effects of Short-Term
1050 Climate Extremes on Isoprene-Emitting and Nonemitting Poplar. *Plant Physiol.* 169: 560-575.

1051 von Caemmerer, S., and Farquhar, G.D. (1981). Some relationships between the
1052 biochemistry of photosynthesis and the gas exchange of leaves. *Planta* 153: 376-387.

1053 Wang, L., Hua, D., He, J., Duan, Y., Chen, Z., Hong, X., and Gong, Z. (2011). Auxin
1054 Response Factor2 (ARF2) and its regulated homeodomain gene HB33 mediate abscisic acid
1055 response in Arabidopsis. *PLoS Genet.* 7: e1002172.

1056 Wang, X., Vignjevic, M., Jiang, D., Jacobsen, S., and Wollenweber, B. (2014). Improved
1057 tolerance to drought stress after anthesis due to priming before anthesis in wheat (*Triticum*
1058 *aestivum* L.) var. Vinjett. *J. Exp. Bot.* 65: 6441-6456.

1059 Warnes, G.R., Bolker, B., Bonebakker, L., Gentleman, R., Huber, W., Liaw, A., Lumley, T.,
1060 Maechler, M., Magnusson, A., Moeller, S., et al. (2016). *gplots: Various R Programming*
1061 *Tools for Plotting Data.*

1062 Wickham, H. (2009). *ggplot2: Elegant Graphics for Data Analysis* (Springer-Verlag New
1063 York).

1064 Wildhagen, H., Paul, S., Allwright, M., Smith, H.K., Malinowska, M., Schnabel, S.K., Paulo,
1065 M.J., Cattonaro, F., Vendramin, V., Scalabrin, S., et al. (2018). Genes and gene clusters
1066 related to genotype and drought-induced variation in saccharification potential, lignin content
1067 and wood anatomical traits in *Populus nigra*. *Tree Physiol* 38: 320-339.

1068 Xu, Z., Zhou, G., and Shimizu, H. (2010). Plant responses to drought and rewatering. *Plant*
1069 *Signal. Behav.* 5: 649-654.

1070 Yao, W., Zhang, X., Zhou, B., Zhao, K., Li, R., and Jiang, T. (2017). Expression Pattern of
1071 ERF Gene Family under Multiple Abiotic Stresses in *Populus simonii* x *P. nigra*. *Front. Plant*
1072 *Sci.* 8: 181.

1073 Yazaki, J., Galli, M., Kim, A.Y., Nito, K., Aleman, F., Chang, K.N., Carvunis, A.R., Quan, R.,
1074 Nguyen, H., Song, L., et al. (2016). Mapping transcription factor interactome networks using
1075 HaloTag protein arrays. *Proc. Natl. Acad. Sci. USA* 113: E4238-4247.

1076 Yu, J., Yang, L., Liu, X., Tang, R., Wang, Y., Ge, H., Wu, M., Zhang, J., Zhao, F., Luan, S., et
1077 al. (2016). Overexpression of Poplar Pyrabactin Resistance-Like Abscisic Acid Receptors
1078 Promotes Abscisic Acid Sensitivity and Drought Resistance in Transgenic Arabidopsis. *PLoS*
1079 *One* 11: e0168040.

1080 Zhang, K., and Gan, S.S. (2012). An abscisic acid-AtNAP transcription factor-SAG113 protein
1081 phosphatase 2C regulatory chain for controlling dehydration in senescing Arabidopsis leaves.
1082 *Plant Physiol.* 158: 961-969.

1083 Zhong, S., Shi, H., Xue, C., Wang, L., Xi, Y., Li, J., Quail, P.H., Deng, X.W., and Guo, H.
1084 (2012). A molecular framework of light-controlled phytohormone action in Arabidopsis. *Curr.*
1085 *Biol.* 22: 1530-1535.

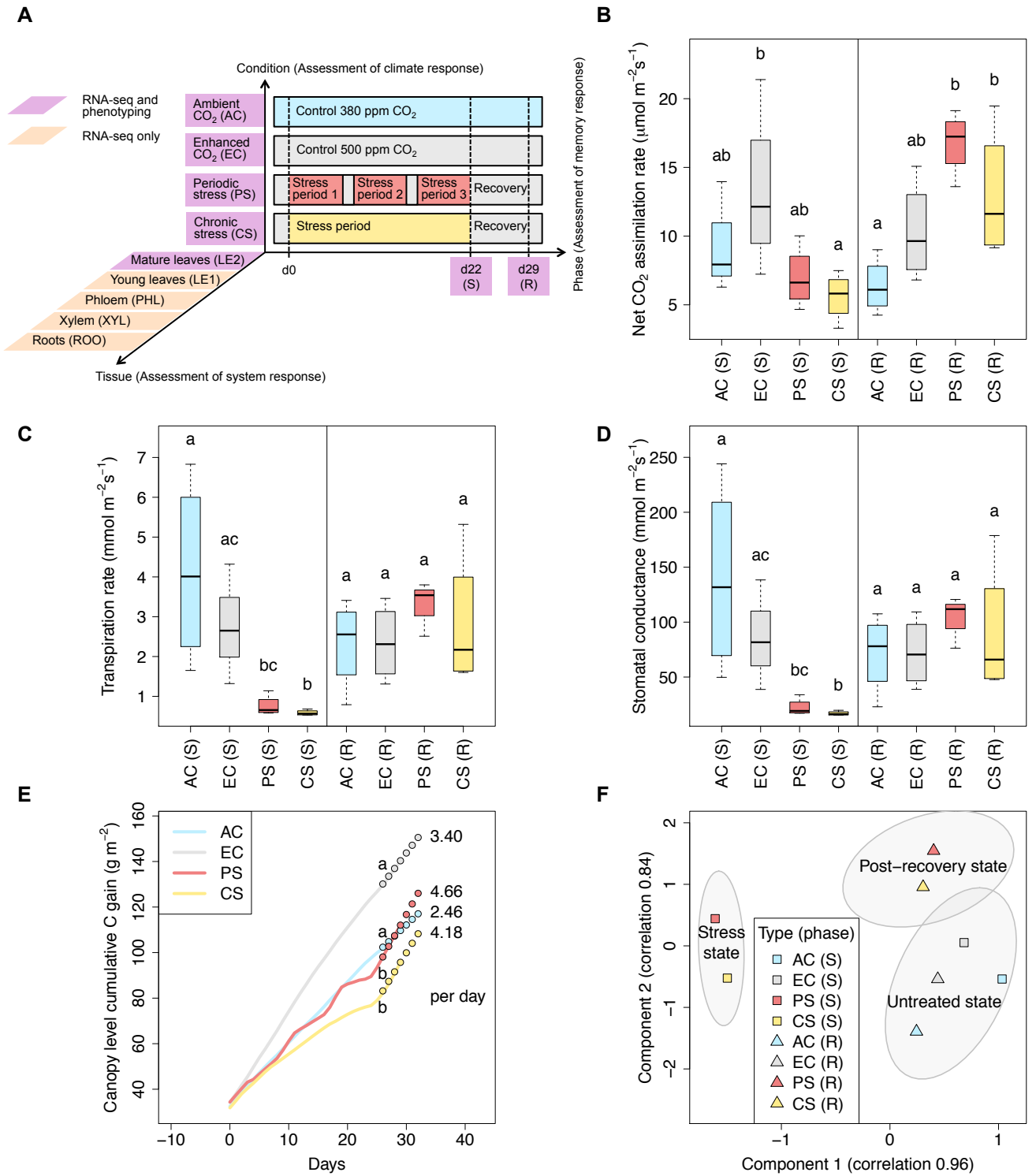


Figure 1. Effect of climatic stress on post-recovery photosynthetic performance of poplar trees. **(A)** The 3D experimental design to investigate climate response of *P. × canescens* trees regarding memory aspects and systemic effects. Plants from four environmental conditions including ambient CO₂ control (AC), enhanced CO₂ control (EC), periodic drought-heat stress (PS) and chronic drought-heat stress (CS) are examined both at the end of a 22-day stress phase (S) and after one week of recovery (R). At the day of the stress treatment start (d0), plants are 8.5 weeks old and already 25 days under AC and EC control climates. For fully developed leaves, both phenotypic and transcriptomic measurements are available, the four other tissues are covered only by transcriptomic data. **(B-D)** Comparison of leaf-level gas exchange rates (leaf no. 9 from the apex) across environmental conditions (Kruskal-Wallis test with posthoc Dunn's test, Benjamini-Hochberg adjustment, p.adj<0.05). **(E)** Carbon gain determined by online gas exchange analysis for the gas-tight sub-chamber of each environmental condition. The slope (shown by circles) is estimated from the last four measurements (day 26 to day 29; Kruskal-Wallis test with posthoc Dunn's test, Benjamini-Hochberg adjustment, p.adj<0.05). **(F)** Projection on the top two components from canonical correlation analysis between gas exchange data and log₂(TPM+1)-transformed per-gene RNA-seq data of the hundred most varying genes in mature leaves across the four conditions and two treatment phases. Each data point represents the mean of biological replicates for the given group; due to destructive harvesting, stress phase RNA-seq measurements were obtained from different biological samples than the continuous gas exchange measurements. Ellipses mark 0.75 confidence levels estimated from the replicates.

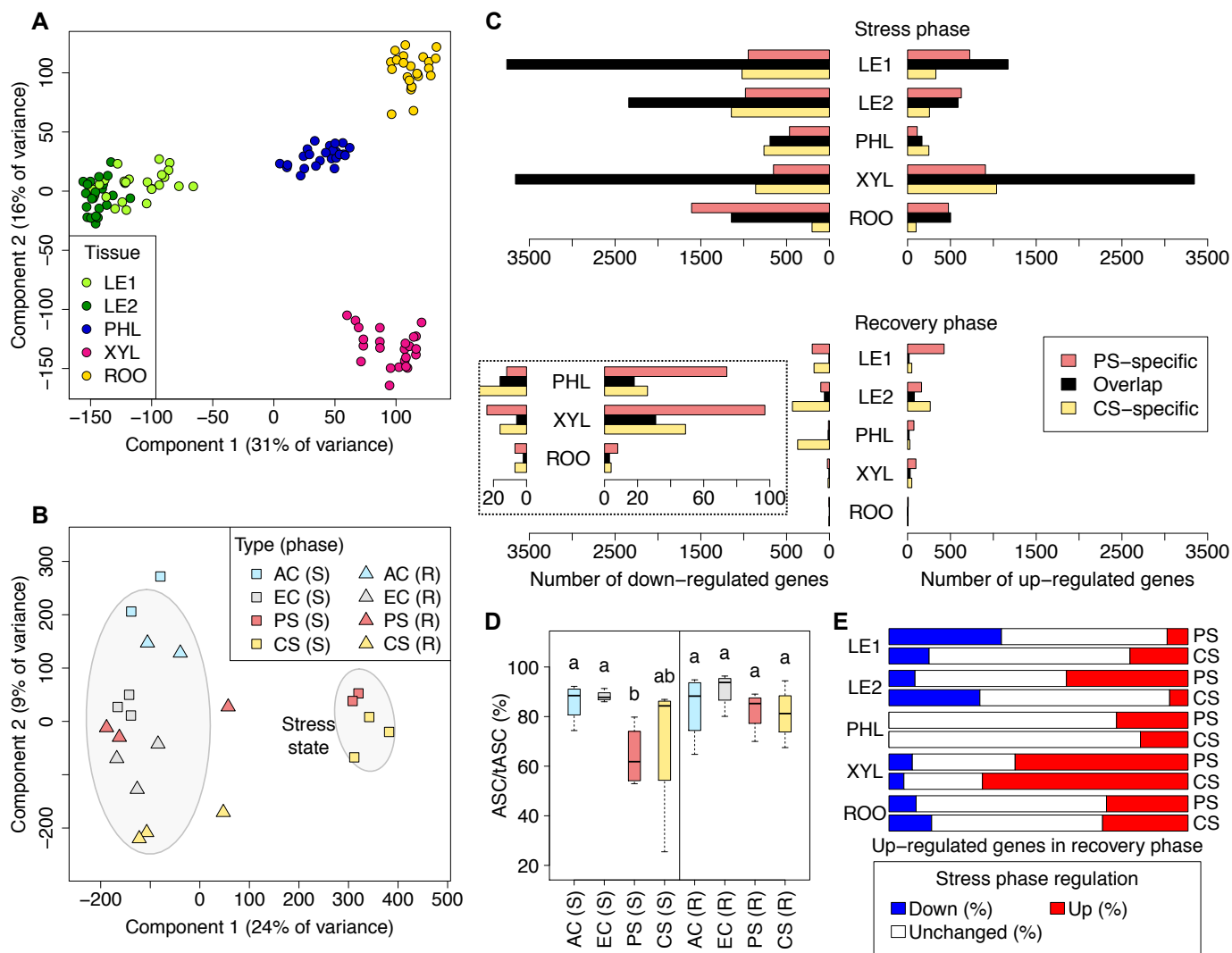


Figure 2. System-wide comparison of poplar gene expression at stress, recovery and control conditions. **(A)** Projection on top two components from principal component analysis of $\log_2(\text{TPM}+1)$ -transformed per-gene RNA-seq data from all samples across four climate conditions, two treatment phases, five different tissues and three biological replicates per group. Data points are colored by tissue (LE1: young leaves, LE2: mature leaves, PHL: phloem, XYL: xylem, ROO: root). **(B)** Principal component analysis of poplar trees with complete RNA-seq measurements from all five tissues, concatenating all tissue measurements from the same tree (Methods). Ellipses mark the 0.75 confidence contour for stressed trees and all other trees (AC: ambient CO_2 , EC: enhanced CO_2 , PS: periodic stress, CS: chronic stress; S: stress phase, R: recovery phase). **(C)** Differentially expressed genes overlapping between periodic (PS) and chronic stress treatment (CS) or unique to each stress type. Differential expression was determined relative to untreated EC controls, for each tissue and treatment phase separately (fold change > 2, $p_{\text{adj}} < 0.05$). The dashed box shows a zoom-in for the three bottommost groups. **(D)** Comparison of antioxidant levels in mature leaves across environmental conditions (Kruskal-Wallis test with posthoc Dunn's test, Benjamini-Hochberg adjustment, $p_{\text{adj}} < 0.05$). The y axis gives the percentage of functional, reduced ascorbate relative to total ascorbate (oxidized and reduced forms). **(E)** Stress-recovery overlap of up-regulated genes. For each tissue, the percentage of stress phase down- or up-regulation of genes up-regulated in the recovery phase relative to control plants is given (fold change > 2, $p_{\text{adj}} < 0.05$).

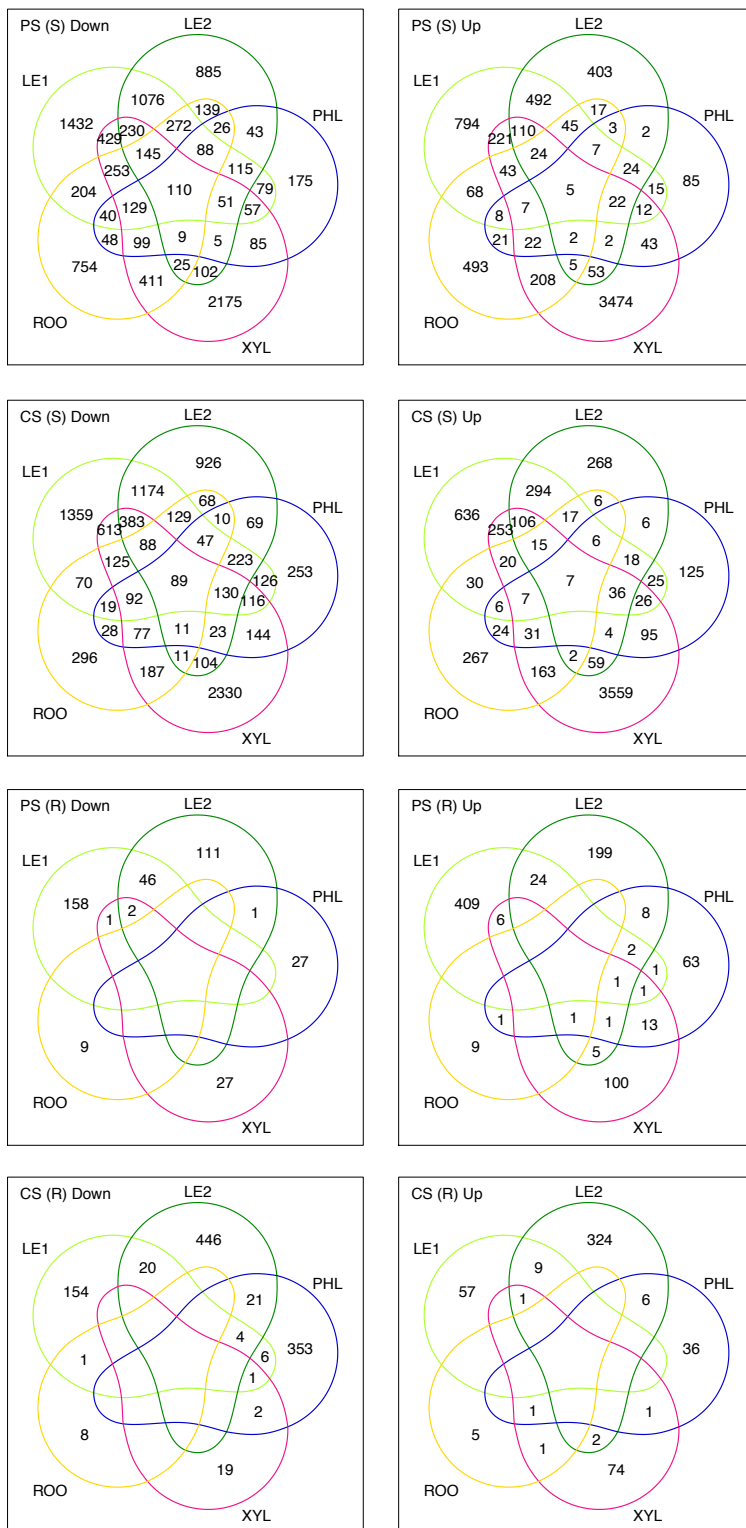


Figure 3. Tissue overlap of differentially expressed poplar genes during stress and recovery phases. Each Venn diagram gives the number of up- or down-regulated genes for a specific treatment type and a specific phase in comparison to untreated controls (LE1: young leaves, LE2: mature leaves, PHL: phloem, XYL: xylem, ROO: root; PS: periodic stress, CS: chronic stress; S: stress phase, R: recovery phase).

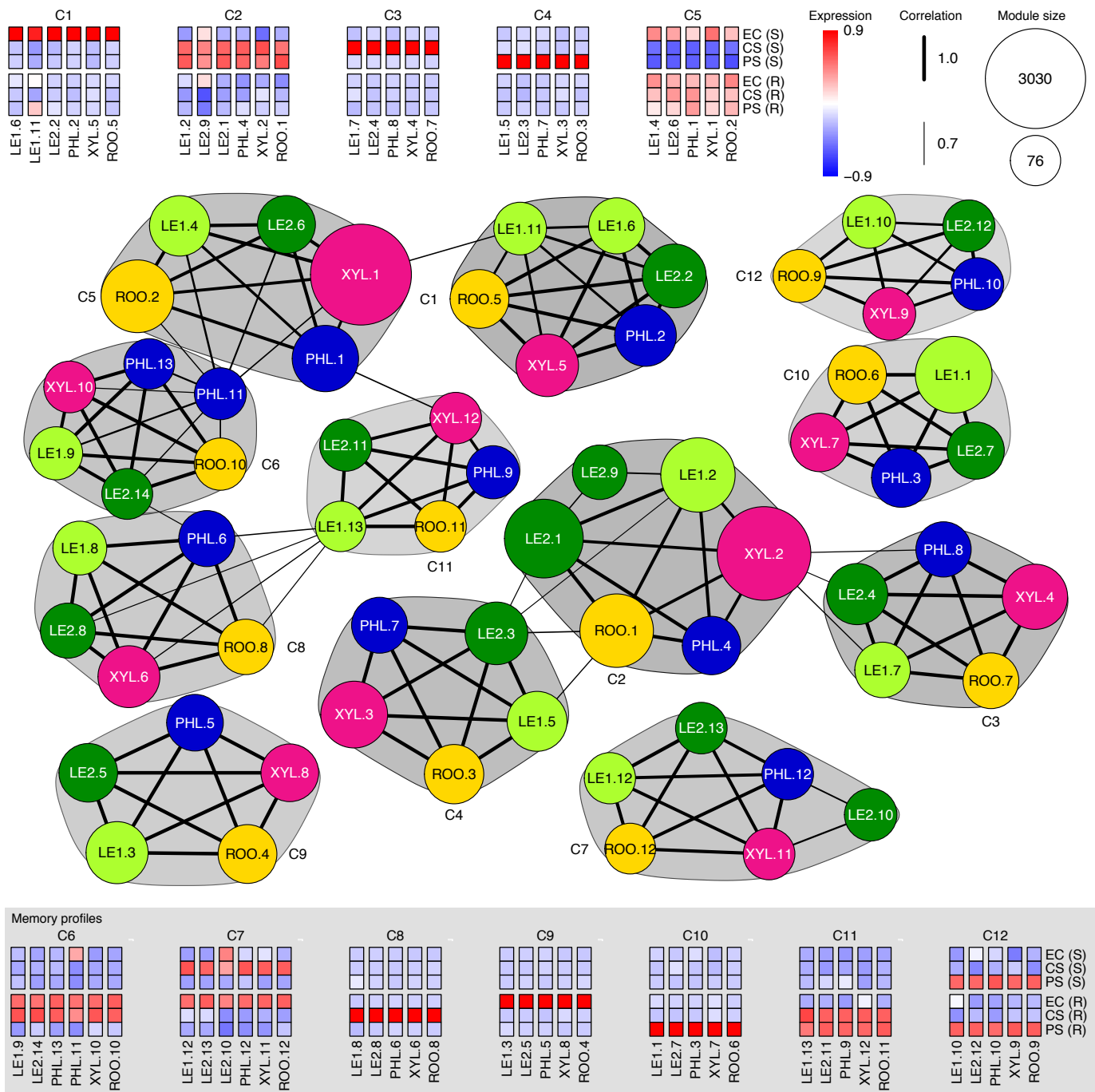
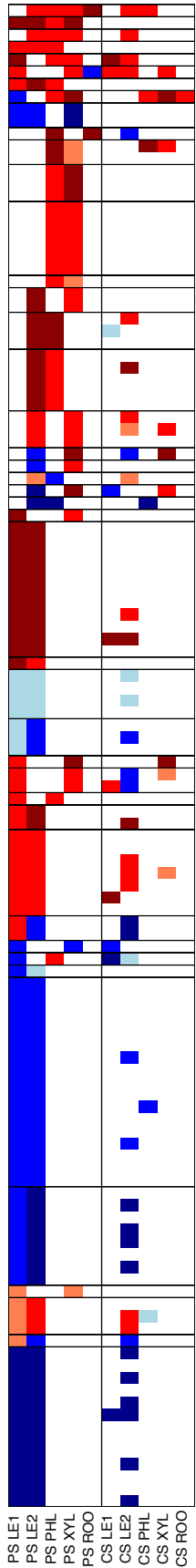
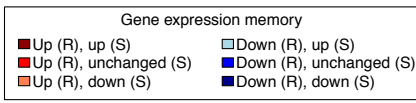


Figure 4. Characteristic poplar gene expression profiles across stress, recovery and control conditions shared by all tissues. Each network node represents a co-expression module of a specific tissue (Methods) indicated by the respective node color (identical code to Fig. 2A) and the prefix of the node label (LE1: young leaves, LE2: mature leaves, PHL: phloem, XYL: xylem, ROO: root). Subsequent numbers in the node label identify the module within each tissue in decreasing order of the module size, which is indicated by node size. Each module is represented by its eigengene profile, which is the first principal component oriented according to average expression. The correlation of module eigengenes was used to cluster modules into communities (Methods). The figure shows all communities that contain modules from all five tissues together with heatmaps of the corresponding eigengenes. Communities are marked by gray polygons and C identifiers (decreasing shades of gray with increasing identifier numbers). For correlation values > 0.7, edges are depicted between module nodes and the edge width represents the correlation strength. The heatmaps with background shading exhibit a pronounced difference between stress-exposed plants and non-treated plants at the end of the recovery phase for at least one stress type, indicative of stress-related memory (EC: elevated CO₂ control, CS: chronic stress, PS: periodic stress; S: stress phase, R: recovery phase). Community C9 putatively represents age-related changes that only occur in non-stressed plants.

A

Potri.005G174400
 Potri.017G009900
 Potri.010G199100
 Potri.004G115600
 Potri.014G106900
 Potri.003G029000
 Potri.003G112600
 Potri.018G139900
 Potri.012G122800
 Potri.017G148800
 Potri.010G150400
 Potri.012G141300
 Potri.015G109100
 Potri.006G093500
 Potri.011G139700
 Potri.013G018000
 Potri.001G192600
 Potri.003G193800
 Potri.005G078700
 Potri.009G151400
 Potri.012G041800
 Potri.014G000400
 Potri.003G141800
 Potri.001G083700
 Potri.012G082800
 Potri.003G131550
 Potri.004G073800
 Potri.013G009200
 Potri.004G074300
 Potri.008G059800
 Potri.008G121900
 Potri.010G184600
 Potri.010G191600
 Potri.001G239650
 Potri.001G239700
 Potri.015G004800
 Potri.003G159800
 Potri.002G220500
 Potri.016G001600
 Potri.008G212400
 Potri.002G094500
 Potri.007G109200
 Potri.001G092100
 Potri.003G129600
 Potri.004G044300
 Potri.005G094900
 Potri.011G129400
 Potri.006G052800
 Potri.008G096500
 Potri.009G107500
 Potri.010G157900
 Potri.010G201400
 Potri.019G131800
 Potri.004G074000
 Potri.001G359200
 Potri.002G027800
 Potri.005G215500
 Potri.009G035100
 Potri.001G191500
 Potri.001G354400
 Potri.010G086200
 Potri.007G088700
 Potri.002G054900
 Potri.006G234900
 Potri.001G235300
 Potri.006G115300
 Potri.011G003200
 Potri.001G099400
 Potri.001G190800
 Potri.003G047700
 Potri.006G089800
 Potri.010G152800
 Potri.0451062800
 Potri.015G097900
 Potri.014G043000
 Potri.009G140400
 Potri.001G408000
 Potri.007G133600
 Potri.003G006800
 Potri.001G347600
 Potri.002G075300
 Potri.003G074500
 Potri.003G089600
 Potri.005G090600
 Potri.009G035000
 Potri.009G044700
 Potri.010G029900
 Potri.010G135100
 Potri.012G008666
 Potri.014G005701
 Potri.014G086900
 Potri.015G098600
 Potri.016G019900
 Potri.017G075700
 Potri.017G083900
 Potri.004G102800
 Potri.005G196700
 Potri.006G127200
 Potri.008G135200
 Potri.010G105700
 Potri.015G002300
 Potri.015G140800
 Potri.017G079000
 Potri.008G100500
 Potri.005G257000
 Potri.006G255800
 Potri.009G005400
 Potri.004G070800
 Potri.001G082150
 Potri.004G072900
 Potri.004G155300
 Potri.007G072600
 Potri.008G131400
 Potri.009G116400
 Potri.012G005900
 Potri.013G119400
 Potri.016G002800
 Potri.016G028900
 Potri.018G142700
 Potri.019G034000
 Potri.T021500

B

Differentially expressed recovery genes relative to EC

● PS-specific ● Overlapping ● CS-specific

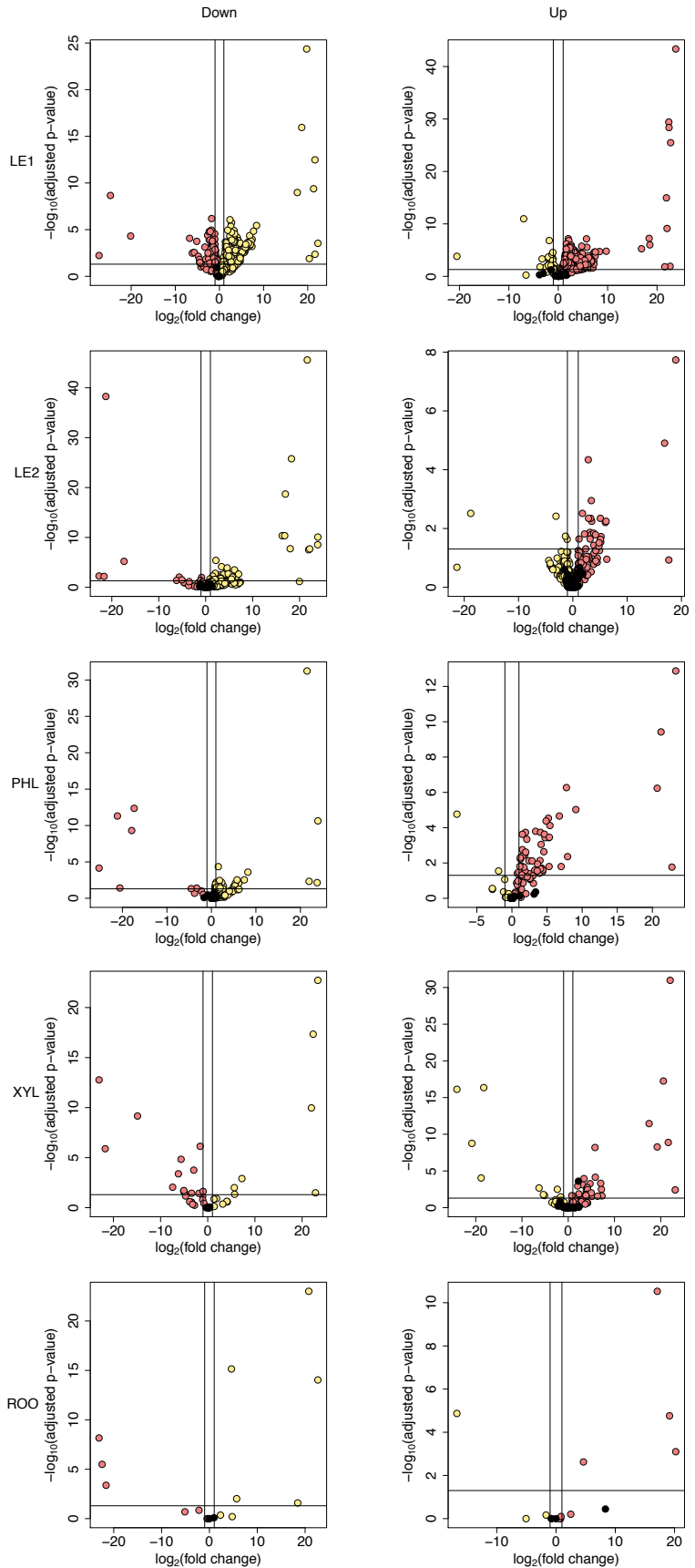


Figure 5. Gene expression memory after recovery from periodic vs. chronic stress. **(A)** Poplar genes with cross-tissue memory responses, i.e. transcriptional up- or down-regulation in post-recovery stress relative to enhanced CO₂ (EC) control samples. The heatmap shows periodic stress (PS) and chronic stress (CS) expression patterns of all genes with PS memory response in at least two tissues (LE1: young leaves, LE2: mature leaves, PHL: phloem, XYL: xylem, ROO: root, R: recovery phase, S: stress phase). **(B)** Direct PS (R) vs. CS (R) comparison of differentially expressed recovery genes determined relative to EC control (see A and Fig. 2C). For each tissue, volcano plots show the distribution of overlapping and stress type-specific differential genes (left: down-regulation, right: up-regulation), taking adjusted p-values and fold changes from the direct comparison. Volcano plots for the respective PS vs. EC and CS vs. EC comparisons are available in Fig. S1.

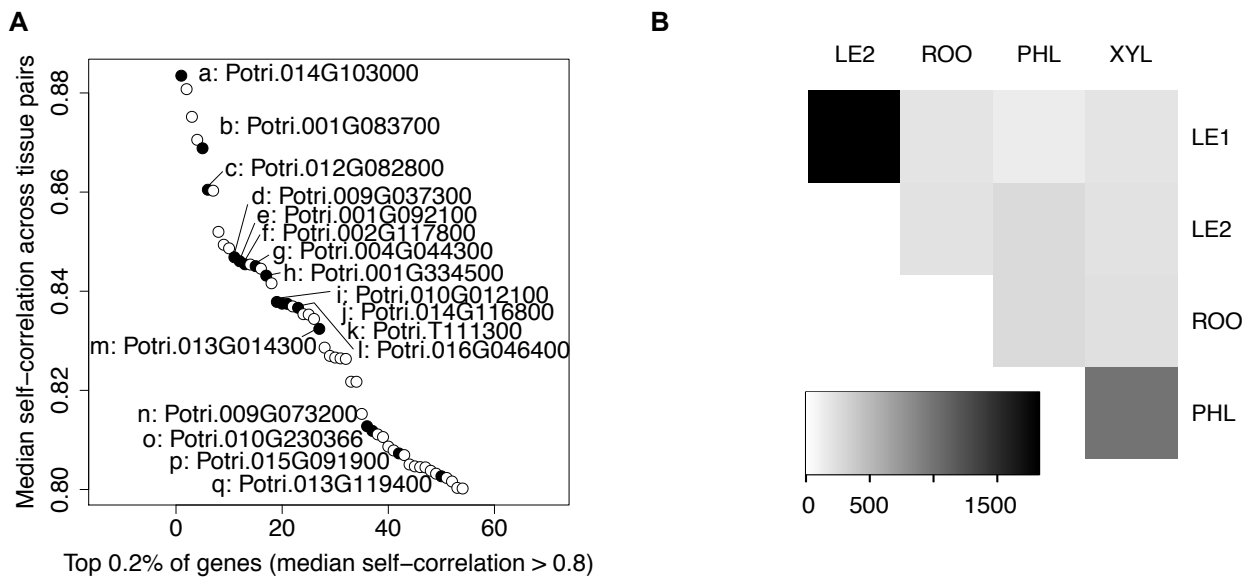


Figure 6. Expression self-correlation of genes across tissues based on fully sampled individual trees. **(A)** The genes with the strongest self-correlation across all tissues. Among them are many genes with periodic stress memory expression pattern in at least one tissue, marked in black and annotated from top to bottom (letters a-q). **(B)** Heatmap showing the number of genes with self-correlation > 0.8 between individual tissues (LE1: young leaves, LE2: mature leaves, PHL: phloem, XYL: xylem, ROO: root).

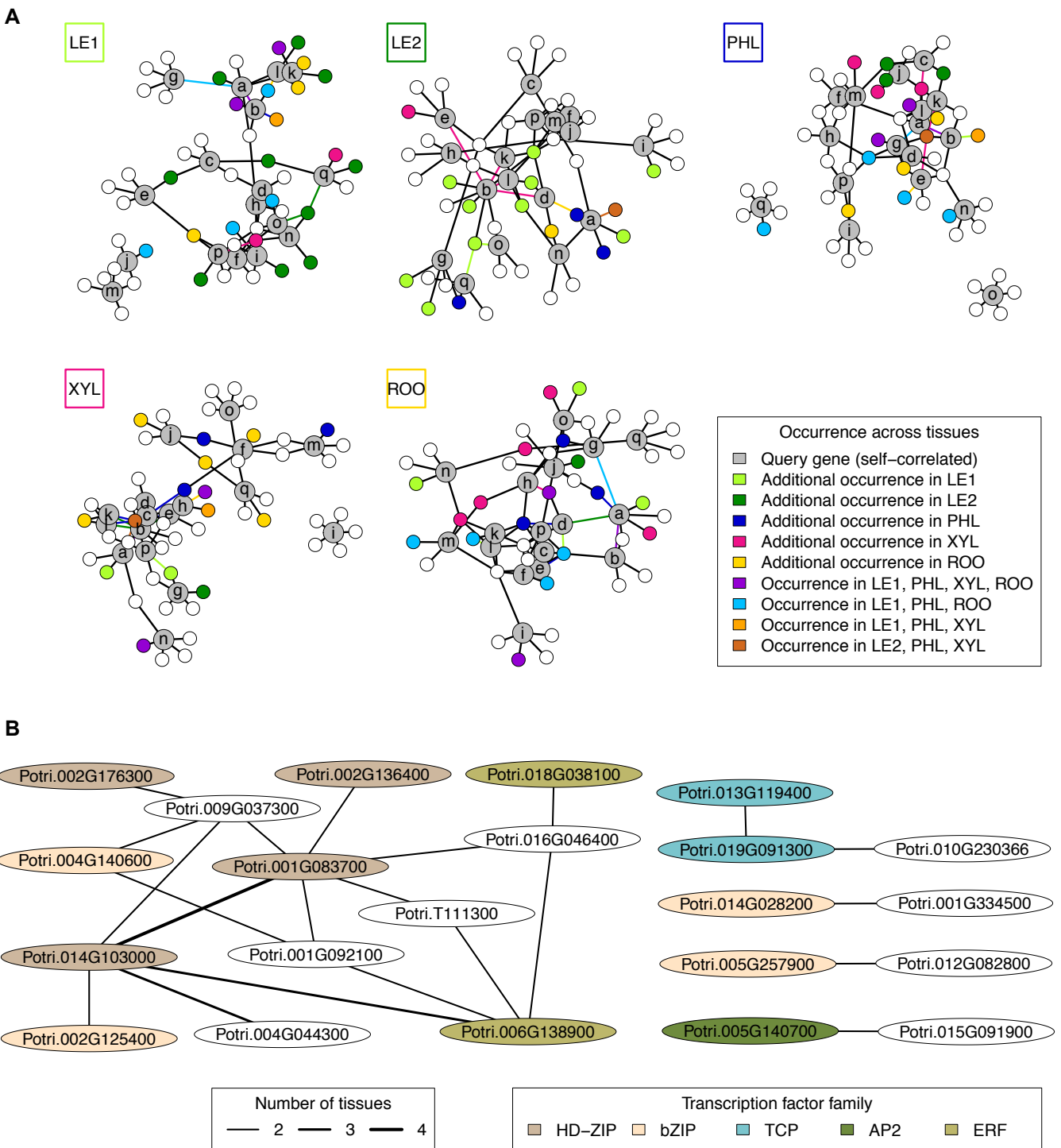
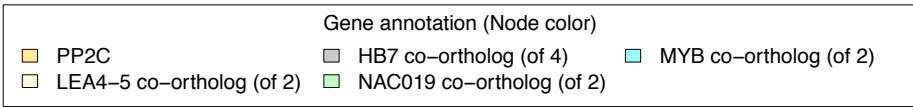
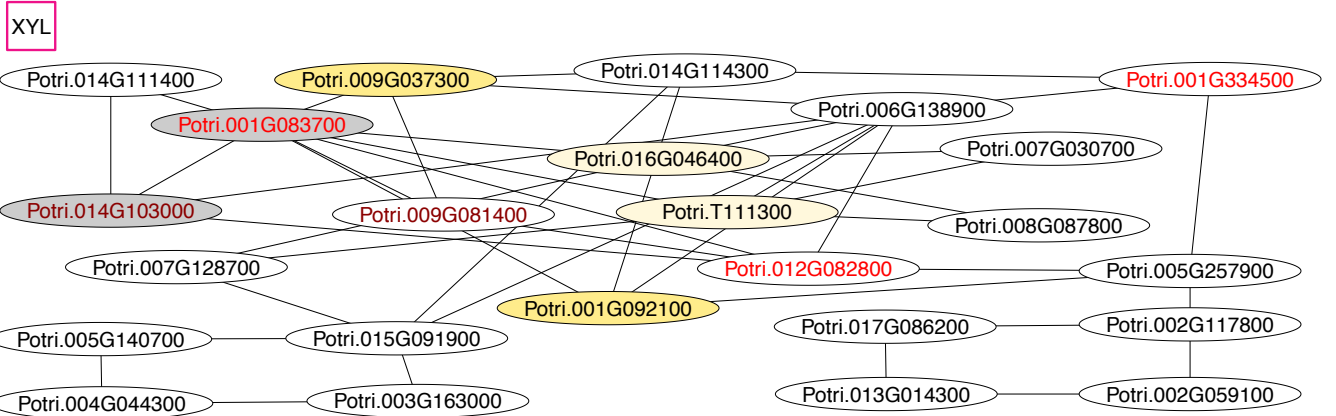
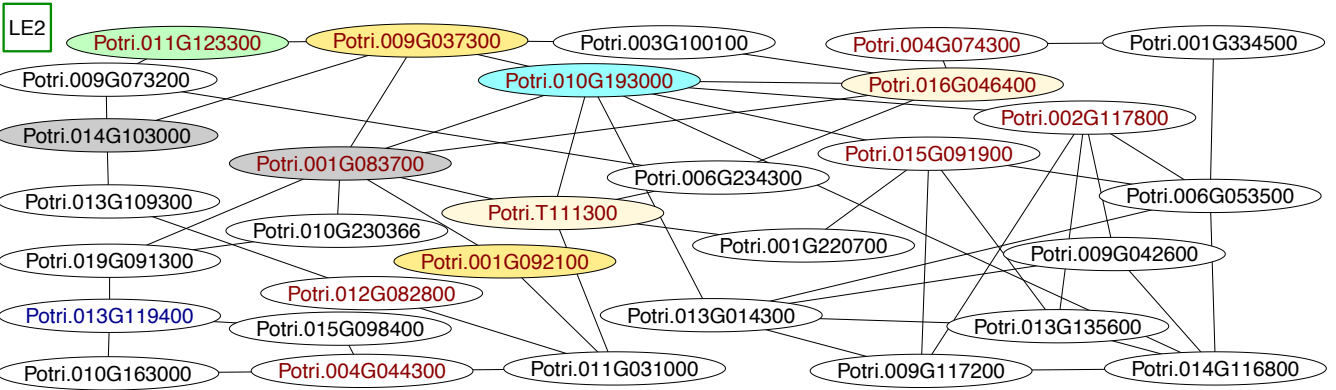
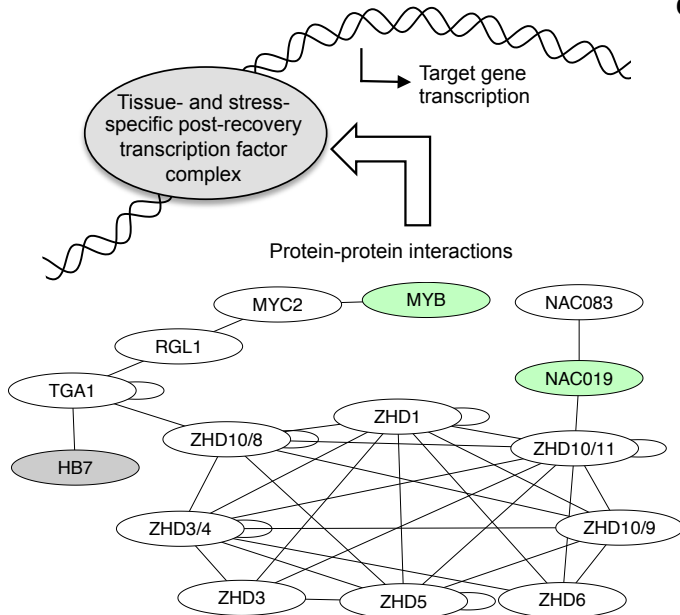


Figure 7. Gene regulatory networks of stress-related multi-tissue memory genes. **(A)** Tissue-specific transcription factor networks around self-correlated genes (gray nodes, labeled by letter code from Fig. 6A). For each tissue network, colored nodes and edges indicate their co-occurrence across several tissue networks (see color key). If nodes or edges occur only in one additional tissue (except the currently considered tissue indicated in the box at the top left of each network), they have the characteristic color of that additional tissue. For example, ten transcription factors occur only in the networks of both young and mature leaves (dark green and light green nodes in the first and second network, respectively). Likewise, nodes q and o are connected to the same transcription factor in these networks (dark green and light green edges in the first and second network, respectively). **(B)** Regulatory relationships co-occurring across tissues. The edge width is proportional to the number of tissues where a specific regulatory relationship was found. Transcription factor nodes are colored according to their transcription factor family.

A



B



C

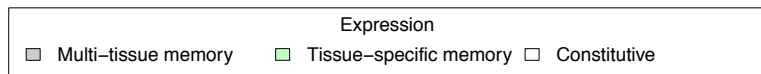
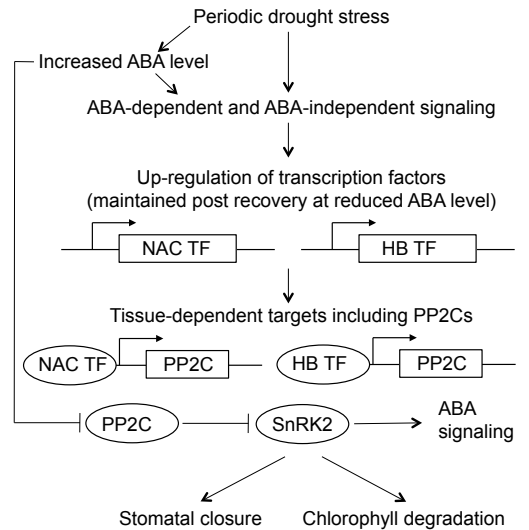


Figure 8. Predicted regulatory stress-related memory processes in mature leaves (LE2) and developing xylem (XYL). **(A)** Core regulatory networks obtained by iteratively removing single-edge nodes from expression-based regulatory network predictions (Fig. 7A). Node label colors refer to periodic stress-related expression patterns. Function annotation is shown for selected nodes discussed in the main text. Potri.010G193000 is a co-ortholog of the *Arabidopsis thaliana* MYB transcription factor AT5G05790, here abbreviated as MYB. **(B)** Model of possible transcription factor complex formation in stress-related memory derived from protein-protein interaction data in *Arabidopsis thaliana*. Gene names are taken from the orthology information in Phytozome. For some ZHD ortholog groups, different *Arabidopsis* genes (marked by an *Arabidopsis* ZHD identifier after the slash) constitute the best BLASTP matches of poplar genes. **(C)** Model suggesting physiological role of protein phosphatases of type 2C (PP2Cs) and regulatory transcription factors in mature leaves during and after periodic stress.

Parsed Citations

AbdElgawad, H., Zinta, G., Hegab, M.M., Pandey, R., Asard, H., and Abuelsoud, W. (2016). High salinity induces different oxidative stress and antioxidant responses in maize seedlings organs. *Front. Plant Sci.* 7: 276.

Pubmed: [Author and Title](#)

Google Scholar: [Author Only Title Only Author and Title](#)

Abraham, P.E., Garcia, B.J., Gunter, L.E., Jawdy, S.S., Engle, N., Yang, X., Jacobson, D.A., Hettich, R.L., Tuskan, G.A., and Tschaplinski, T.J. (2018). Quantitative proteome profile of water deficit stress responses in eastern cottonwood (*Populus deltoides*) leaves. *PLoS One* 13: e0190019.

Pubmed: [Author and Title](#)

Google Scholar: [Author Only Title Only Author and Title](#)

Aibar, S., Gonzalez-Bias, C.B., Moerman, T., Huynh-Thu, V.A., Imrichova, H., Hulselmans, G., Rambow, F., Marine, J.C., Geurts, P., Aerts, J., et al. (2017). SCENIC: single-cell regulatory network inference and clustering. *Nat. Methods* 14: 1083-1086.

Pubmed: [Author and Title](#)

Google Scholar: [Author Only Title Only Author and Title](#)

Arabidopsis Interactome Mapping Consortium (2011). Evidence for network evolution in an Arabidopsis interactome map. *Science* 333: 601-607.

Pubmed: [Author and Title](#)

Google Scholar: [Author Only Title Only Author and Title](#)

Ariel, F.D., Manavella, P.A., Dezar, C.A., and Chan, R.L. (2007). The true story of the HD-Zip family. *Trends Plant Sci.* 12: 419-426.

Pubmed: [Author and Title](#)

Google Scholar: [Author Only Title Only Author and Title](#)

Aroca, R., Porcel, R., and Ruiz-Lozano, J.M. (2012). Regulation of root water uptake under abiotic stress conditions. *J. Exp. Bot.* 63: 43-57.

Pubmed: [Author and Title](#)

Google Scholar: [Author Only Title Only Author and Title](#)

Asensi-Fabado, M.A., Amtmann, A., and Perrella, G. (2017). Plant responses to abiotic stress: The chromatin context of transcriptional regulation. *Biochim. Biophys. Acta* 1860: 106-122.

Pubmed: [Author and Title](#)

Google Scholar: [Author Only Title Only Author and Title](#)

Auguie, B. (2017). gridExtra: Miscellaneous Functions for "Grid" Graphics.

Battaglia, M., Olvera-Carrillo, Y., Garcarrubio, A., Campos, F., and Covarrubias, A.A. (2008). The enigmatic LEA proteins and other hydrophilins. *Plant Physiol.* 148: 6-24.

Pubmed: [Author and Title](#)

Google Scholar: [Author Only Title Only Author and Title](#)

Berardini, T.Z., Reiser, L., Li, D., Mezheritsky, Y., Muller, R., Strait, E., and Huala, E. (2015). The Arabidopsis information resource: Making and mining the "gold standard" annotated reference plant genome. *Genesis* 53: 474-485.

Pubmed: [Author and Title](#)

Google Scholar: [Author Only Title Only Author and Title](#)

Bi, Z., Merl-Pham, J., Uehlein, N., Zimmer, I., Mühlhans, S., Aichler, M., Walch, A.K., Kaldenhoff, R., Palme, K., Schnitzler, J.P., et al. (2015). RNAi-mediated downregulation of poplar plasma membrane intrinsic proteins (PIPs) changes plasma membrane proteome composition and affects leaf physiology. *J. Proteomics* 128: 321-332.

Pubmed: [Author and Title](#)

Google Scholar: [Author Only Title Only Author and Title](#)

Bloemen, J., Vergeynst, L.L., Overlaet-Michiels, L., and Steppe, K. (2016). How important is woody tissue photosynthesis in poplar during drought stress? *Trees* 30: 63-72.

Pubmed: [Author and Title](#)

Google Scholar: [Author Only Title Only Author and Title](#)

Challa, K.R., Aggarwal, P., and Nath, U. (2016). Activation of YUCCA5 by the Transcription Factor TCP4 Integrates Developmental and Environmental Signals to Promote Hypocotyl Elongation in Arabidopsis. *Plant Cell.*

Pubmed: [Author and Title](#)

Google Scholar: [Author Only Title Only Author and Title](#)

Chen, J., Zhang, D., Zhang, C., Xia, X., Yin, W., and Tian, Q. (2015). A Putative PP2C-Encoding Gene Negatively Regulates ABA Signaling in *Populus euphratica*. *PLoS One* 10: e0139466.

Pubmed: [Author and Title](#)

Google Scholar: [Author Only Title Only Author and Title](#)

Crisp, P.A., Ganguly, D., Eichten, S.R., Borevitz, J.O., and Pogson, B.J. (2016). Reconsidering plant memory: Intersections between stress recovery, RNA turnover, and epigenetics. *Sci. Adv.* 2: e1501340.

Pubmed: [Author and Title](#)

Google Scholar: [Author Only Title Only Author and Title](#)

Csardi, G., and Nepusz, T. (2006). The igraph software package for complex network research. *InterJournal Complex Systems*: 1695.

Pubmed: [Author and Title](#)

Google Scholar: [Author Only Title Only Author and Title](#)

Ding, Y., Fromm, M., and Avramova, Z. (2012). Multiple exposures to drought 'train' transcriptional responses in *Arabidopsis*. *Nat Commun* 3: 740.

Pubmed: [Author and Title](#)

Google Scholar: [Author Only Title Only Author and Title](#)

Ding, Y., Liu, N., Virlouvet, L., Riethoven, J.J., Fromm, M., and Avramova, Z. (2013). Four distinct types of dehydration stress memory genes in *Arabidopsis thaliana*. *BMC Plant Biol.* 13: 229.

Pubmed: [Author and Title](#)

Google Scholar: [Author Only Title Only Author and Title](#)

Dong, C.J., and Liu, J.Y. (2010). The *Arabidopsis* EAR-motif-containing protein RAP2.1 functions as an active transcriptional repressor to keep stress responses under tight control. *BMC Plant Biol.* 10: 47.

Pubmed: [Author and Title](#)

Google Scholar: [Author Only Title Only Author and Title](#)

Dupeux, F., Antoni, R., Betz, K., Santiago, J., Gonzalez-Guzman, M., Rodriguez, L., Rubio, S., Park, S.Y., Cutler, S.R., Rodriguez, P.L., et al. (2011). Modulation of abscisic acid signaling in vivo by an engineered receptor-insensitive protein phosphatase type 2C allele. *Plant Physiol.* 156: 106-116.

Pubmed: [Author and Title](#)

Google Scholar: [Author Only Title Only Author and Title](#)

Dusa, A. (2018). venn: Draw Venn Diagrams.

Fleta-Soriano, E., and Munne-Bosch, S. (2016). Stress Memory and the Inevitable Effects of Drought: A Physiological Perspective. *Front. Plant Sci.* 7: 143.

Pubmed: [Author and Title](#)

Google Scholar: [Author Only Title Only Author and Title](#)

Fox, J., and Weisberg, S. (2011). An R Companion to Applied Regression (Sage).

Fuchs, S., Grill, E., Meskiene, I., and Schweighofer, A. (2013). Type 2C protein phosphatases in plants. *FEBS J.* 280: 681-693.

Pubmed: [Author and Title](#)

Google Scholar: [Author Only Title Only Author and Title](#)

Fujii, H., Verslues, P.E., and Zhu, J.K. (2011). *Arabidopsis* decuple mutant reveals the importance of SnRK2 kinases in osmotic stress responses in vivo. *Proc Natl Acad Sci U S A* 108: 1717-1722.

Pubmed: [Author and Title](#)

Google Scholar: [Author Only Title Only Author and Title](#)

Gansner, E.R., and North, S.C. (2000). An open graph visualization system and its applications to software engineering. *SOFTWARE - PRACTICE AND EXPERIENCE* 30: 1203-1233.

Pubmed: [Author and Title](#)

Google Scholar: [Author Only Title Only Author and Title](#)

Gao, S., Gao, J., Zhu, X., Song, Y., Li, Z., Ren, G., Zhou, X., and Kuai, B. (2016). ABF2, ABF3, and ABF4 Promote ABA-Mediated Chlorophyll Degradation and Leaf Senescence by Transcriptional Activation of Chlorophyll Catabolic Genes and Senescence-Associated Genes in *Arabidopsis*. *Mol Plant* 9: 1272-1285.

Pubmed: [Author and Title](#)

Google Scholar: [Author Only Title Only Author and Title](#)

Gonzalez, I., Le Cao, K.A., and Dejean, S. (2011). mixOmics: Omics data integration project.

Goodstein, D.M., Shu, S., Howson, R., Neupane, R., Hayes, R.D., Fazo, J., Mitros, T., Dirks, W., Hellsten, U., Putnam, N., et al. (2012). *Phytozome*: a comparative platform for green plant genomics. *Nucleic Acids Res.* 40: D1178-1186.

Pubmed: [Author and Title](#)

Google Scholar: [Author Only Title Only Author and Title](#)

Hagedorn, F., Joseph, J., Peter, M., Luster, J., Pritsch, K., Geppert, U., Kerner, R., Molinier, V., Egli, S., Schaub, M., et al. (2016). Recovery of trees from drought depends on belowground sink control. *Nat. Plants* 2: 16111.

Pubmed: [Author and Title](#)

Google Scholar: [Author Only Title Only Author and Title](#)

Harfouche, A., Meilan, R., and Altman, A. (2014). Molecular and physiological responses to abiotic stress in forest trees and their relevance to tree improvement. *Tree Physiol* 34: 1181-1198.

Pubmed: [Author and Title](#)

Google Scholar: [Author Only Title Only Author and Title](#)

Hilker, M., Schwachtje, J., Baier, M., Balazadeh, S., Baurle, I., Geiselhardt, S., Hinch, D.K., Kunze, R., Mueller-Roeber, B., Rillig, M.C., et al. (2016). Priming and memory of stress responses in organisms lacking a nervous system. *Biol. Rev. Camb. Philos. Soc.* 91: 1118-1133.

- Pubmed: [Author and Title](#)
Google Scholar: [Author Only Title Only Author and Title](#)
- Hjellström, M., Olsson, A.S.B., Engström, O., and Söderman, E.M. (2003). Constitutive expression of the water deficit-inducible homeobox gene ATHB7 in transgenic Arabidopsis causes a suppression of stem elongation growth. *Plant Cell Environ.* 26: 1127-1136.
Pubmed: [Author and Title](#)
Google Scholar: [Author Only Title Only Author and Title](#)
- Huynh-Thu, V.A., Irrthum, A., Wehenkel, L., and Geurts, P. (2010). Inferring regulatory networks from expression data using tree-based methods. *PLoS One* 5.
Pubmed: [Author and Title](#)
Google Scholar: [Author Only Title Only Author and Title](#)
- International Barley Genome Sequencing Consortium, Mayer, K.F., Waugh, R., Brown, J.W., Schulman, A., Langridge, P., Platzer, M., Fincher, G.B., Muehlbauer, G.J., Sato, K., et al. (2012). A physical, genetic and functional sequence assembly of the barley genome. *Nature* 491: 711-716.
Pubmed: [Author and Title](#)
Google Scholar: [Author Only Title Only Author and Title](#)
- IPCC (2014). Near-term Climate Change: Projections and Predictability. In *Climate Change 2013: The Physical Science Basis. Contribution of Working Group I to the Fifth Assessment Report of the Intergovernmental Panel on Climate Change*, T.F. Stocker, D. Qin, G.K. Plattner, M. Tignor, S.K. Allen, J. Boschung, A. Nauels, Y. Xia, B. V., and P.M. Midgley, eds. (Cambridge: Cambridge University Press).
Pubmed: [Author and Title](#)
Google Scholar: [Author Only Title Only Author and Title](#)
- Jin, J., Zhang, H., Kong, L., Gao, G., and Luo, J. (2014). PlantTFDB 3.0: a portal for the functional and evolutionary study of plant transcription factors. *Nucleic Acids Res.* 42: D1182-1187.
Pubmed: [Author and Title](#)
Google Scholar: [Author Only Title Only Author and Title](#)
- Jud, W., Vanzo, E., Li, Z., Ghirardo, A., Zimmer, I., Sharkey, T.D., Hansel, A., and Schnitzler, J.P. (2016). Effects of heat and drought stress on post-illumination bursts of volatile organic compounds in isoprene-emitting and non-emitting poplar. *Plant Cell Environ.* 39: 1204-1215.
Pubmed: [Author and Title](#)
Google Scholar: [Author Only Title Only Author and Title](#)
- Kim, D., Perte, G., Trapnell, C., Pimentel, H., Kelley, R., and Salzberg, S.L. (2013). TopHat2: accurate alignment of transcriptomes in the presence of insertions, deletions and gene fusions. *Genome Biol.* 14: R36.
Pubmed: [Author and Title](#)
Google Scholar: [Author Only Title Only Author and Title](#)
- Kim, M., Lee, U., Small, I., des Francs-Small, C.C., and Vierling, E. (2012). Mutations in an Arabidopsis mitochondrial transcription termination factor-related protein enhance thermotolerance in the absence of the major molecular chaperone HSP101. *Plant Cell* 24: 3349-3365.
Pubmed: [Author and Title](#)
Google Scholar: [Author Only Title Only Author and Title](#)
- Kolde, R. (2018). pheatmap: Pretty Heatmaps.**
- Kotak, S., Larkindale, J., Lee, U., von Koskull-Doring, P., Vierling, E., and Scharf, K.D. (2007). Complexity of the heat stress response in plants. *Curr. Opin. Plant Biol.* 10: 310-316.
Pubmed: [Author and Title](#)
Google Scholar: [Author Only Title Only Author and Title](#)
- Kulik, A., Wawer, I., Krzywinska, E., Bucholc, M., and Dobrowolska, G. (2011). SnRK2 protein kinases—key regulators of plant response to abiotic stresses. *OMICS* 15: 859-872.
Pubmed: [Author and Title](#)
Google Scholar: [Author Only Title Only Author and Title](#)
- Länke, J., Brzezinka, K., Altmann, S., and Bäurle, I. (2016). A hit-and-run heat shock factor governs sustained histone methylation and transcriptional stress memory. *EMBO J.* 35: 162-175.
Pubmed: [Author and Title](#)
Google Scholar: [Author Only Title Only Author and Title](#)
- Langfelder, P., and Horvath, S. (2007). Eigengene networks for studying the relationships between co-expression modules. *BMC Syst. Biol.* 1: 54.
Pubmed: [Author and Title](#)
Google Scholar: [Author Only Title Only Author and Title](#)
- Langfelder, P., and Horvath, S. (2008). WGCNA: an R package for weighted correlation network analysis. *BMC Bioinformatics* 9: 559.
Pubmed: [Author and Title](#)
Google Scholar: [Author Only Title Only Author and Title](#)
- Langfelder, P., and Horvath, S. (2012). Fast R Functions for Robust Correlations and Hierarchical Clustering. *J Stat Softw* 46.

- Pubmed: [Author and Title](#)
Google Scholar: [Author Only Title Only Author and Title](#)
- Langfelder, P., Zhang, B., and Horvath, S. (2008).** Defining clusters from a hierarchical cluster tree: the Dynamic Tree Cut package for R. *Bioinformatics* 24: 719-720.
Pubmed: [Author and Title](#)
Google Scholar: [Author Only Title Only Author and Title](#)
- Le Cao, K.A., Gonzalez, I., and Dejean, S. (2009).** integrOmics: an R package to unravel relationships between two omics datasets. *Bioinformatics* 25: 2855-2856.
Pubmed: [Author and Title](#)
Google Scholar: [Author Only Title Only Author and Title](#)
- Leonhardt, N., Kwak, J.M., Robert, N., Waner, D., Leonhardt, G., and Schroeder, J.I. (2004).** Microarray expression analyses of Arabidopsis guard cells and isolation of a recessive abscisic acid hypersensitive protein phosphatase 2C mutant. *Plant Cell* 16: 596-615.
Pubmed: [Author and Title](#)
Google Scholar: [Author Only Title Only Author and Title](#)
- Leple, J.C., Brasileiro, A.C., Michel, M.F., Delmotte, F., and Jouanin, L. (1992).** Transgenic poplars: expression of chimeric genes using four different constructs. *Plant Cell Rep.* 11: 137-141.
Pubmed: [Author and Title](#)
Google Scholar: [Author Only Title Only Author and Title](#)
- Li, S. (2014).** Redox Modulation Matters: Emerging Functions for Glutaredoxins in Plant Development and Stress Responses. *Plants (Basel)* 3: 559-582.
Pubmed: [Author and Title](#)
Google Scholar: [Author Only Title Only Author and Title](#)
- Lippold, F., vom Dorp, K., Abraham, M., Holzl, G., Wewer, V., Yilmaz, J.L., Lager, I., Montandon, C., Besagni, C., Kessler, F., et al. (2012).** Fatty acid phytyl ester synthesis in chloroplasts of Arabidopsis. *Plant Cell* 24: 2001-2014.
Pubmed: [Author and Title](#)
Google Scholar: [Author Only Title Only Author and Title](#)
- Liu, N., Staswick, P.E., and Avramova, Z. (2016).** Memory responses of jasmonic acid-associated Arabidopsis genes to a repeated dehydration stress. *Plant Cell Environ.* 39: 2515-2529.
Pubmed: [Author and Title](#)
Google Scholar: [Author Only Title Only Author and Title](#)
- Love, M.I., Huber, W., and Anders, S. (2014).** Moderated estimation of fold change and dispersion for RNA-seq data with DESeq2. *Genome Biol.* 15: 550.
Pubmed: [Author and Title](#)
Google Scholar: [Author Only Title Only Author and Title](#)
- Mi, H., Huang, X., Muruganujan, A., Tang, H., Mills, C., Kang, D., and Thomas, P.D. (2017).** PANTHER version 11: expanded annotation data from Gene Ontology and Reactome pathways, and data analysis tool enhancements. *Nucleic Acids Res.* 45: D183-D189.
Pubmed: [Author and Title](#)
Google Scholar: [Author Only Title Only Author and Title](#)
- Nakashima, K., Fujita, Y., Kanamori, N., Katagiri, T., Umezawa, T., Kidokoro, S., Maruyama, K., Yoshida, T., Ishiyama, K., Kobayashi, M., et al. (2009).** Three Arabidopsis SnRK2 protein kinases, SRK2D/SnRK2.2, SRK2E/SnRK2.6/OST1 and SRK2I/SnRK2.3, involved in ABA signaling are essential for the control of seed development and dormancy. *Plant Cell Physiol.* 50: 1345-1363.
Pubmed: [Author and Title](#)
Google Scholar: [Author Only Title Only Author and Title](#)
- Nakashima, K., Yamaguchi-Shinozaki, K., and Shinozaki, K. (2014).** The transcriptional regulatory network in the drought response and its crosstalk in abiotic stress responses including drought, cold, and heat. *Front. Plant Sci.* 5: 170.
Pubmed: [Author and Title](#)
Google Scholar: [Author Only Title Only Author and Title](#)
- Olvera-Carrillo, Y., Campos, F., Reyes, J.L., Garcarrubio, A., and Covarrubias, AA (2010).** Functional analysis of the group 4 late embryogenesis abundant proteins reveals their relevance in the adaptive response during water deficit in Arabidopsis. *Plant Physiol.* 154: 373-390.
Pubmed: [Author and Title](#)
Google Scholar: [Author Only Title Only Author and Title](#)
- Osakabe, Y., Osakabe, K., Shinozaki, K., and Tran, L.S. (2014).** Response of plants to water stress. *Front. Plant Sci.* 5: 86.
Pubmed: [Author and Title](#)
Google Scholar: [Author Only Title Only Author and Title](#)
- Paul, S., Wildhagen, H., Janz, D., and Polle, A. (2018).** Drought effects on the tissue- and cell-specific cytokinin activity in poplar. *AoB Plants* 10: plx067.
Pubmed: [Author and Title](#)
Google Scholar: [Author Only Title Only Author and Title](#)

Pertea, M., Pertea, G.M., Antonescu, C.M., Chang, T.C., Mendell, J.T., and Salzberg, S.L. (2015). StringTie enables improved reconstruction of a transcriptome from RNA-seq reads. *Nat. Biotechnol.* 33: 290-295.

Pubmed: [Author and Title](#)

Google Scholar: [Author Only](#) [Title Only](#) [Author and Title](#)

Pfanz, H., Aschan, G., Langenfeld-Heyser, R., Wittmann, C., and Loose, M. (2002). Ecology and ecophysiology of tree stems: corticular and wood photosynthesis. *Naturwissenschaften* 89: 147-162.

Pubmed: [Author and Title](#)

Google Scholar: [Author Only](#) [Title Only](#) [Author and Title](#)

R Core Team (2018). R: A Language and Environment for Statistical Computing.

Re, D.A., Capella, M., Bonaventure, G., and Chan, R.L. (2014). *Arabidopsis* AtHB7 and AtHB12 evolved divergently to fine tune processes associated with growth and responses to water stress. *BMC Plant Biol.* 14: 150.

Pubmed: [Author and Title](#)

Google Scholar: [Author Only](#) [Title Only](#) [Author and Title](#)

Samol, I., Shapiguzov, A., Ingelsson, B., Fucile, G., Crevecoeur, M., Vener, A.V., Rochaix, J.D., and Goldschmidt-Clermont, M. (2012). Identification of a photosystem II phosphatase involved in light acclimation in *Arabidopsis*. *Plant Cell* 24: 2596-2609.

Pubmed: [Author and Title](#)

Google Scholar: [Author Only](#) [Title Only](#) [Author and Title](#)

Sani, E., Herzyk, P., Perrella, G., Colot, V., and Amtmann, A. (2013). Hyperosmotic priming of *Arabidopsis* seedlings establishes a long-term somatic memory accompanied by specific changes of the epigenome. *Genome Biol.* 14: R59.

Pubmed: [Author and Title](#)

Google Scholar: [Author Only](#) [Title Only](#) [Author and Title](#)

Schäfer, J., and Strimmer, K. (2005). A shrinkage approach to large-scale covariance matrix estimation and implications for functional genomics. *Stat Appl Genet Mol Biol* 4: Article32.

Pubmed: [Author and Title](#)

Google Scholar: [Author Only](#) [Title Only](#) [Author and Title](#)

Scholander, P.F., Bradstreet, E.D., Hemmingsen, E.A., and Hammel, H.T. (1965). Sap Pressure in Vascular Plants: Negative hydrostatic pressure can be measured in plants. *Science* 148: 339-346.

Pubmed: [Author and Title](#)

Google Scholar: [Author Only](#) [Title Only](#) [Author and Title](#)

Shinozaki, K., and Yamaguchi-Shinozaki, K. (2007). Gene networks involved in drought stress response and tolerance. *J. Exp. Bot.* 58: 221-227.

Pubmed: [Author and Title](#)

Google Scholar: [Author Only](#) [Title Only](#) [Author and Title](#)

Singh, D., and Laxmi, A. (2015). Transcriptional regulation of drought response: a tortuous network of transcriptional factors. *Front. Plant Sci.* 6: 895.

Pubmed: [Author and Title](#)

Google Scholar: [Author Only](#) [Title Only](#) [Author and Title](#)

Söderman, E., Mattsson, J., and Engström, P. (1996). The *Arabidopsis* homeobox gene ATHB-7 is induced by water deficit and by abscisic acid. *Plant J.* 10: 375-381.

Pubmed: [Author and Title](#)

Google Scholar: [Author Only](#) [Title Only](#) [Author and Title](#)

Soy, J., Leivar, P., Gonzalez-Schain, N., Sentandreu, M., Prat, S., Quail, P.H., and Monte, E. (2012). Phytochrome-imposed oscillations in PIF3 protein abundance regulate hypocotyl growth under diurnal light/dark conditions in *Arabidopsis*. *Plant J.* 71: 390-401.

Pubmed: [Author and Title](#)

Google Scholar: [Author Only](#) [Title Only](#) [Author and Title](#)

Sun, X., Wang, C., Xiang, N., Li, X., Yang, S., Du, J., Yang, Y., and Yang, Y. (2017). Activation of secondary cell wall biosynthesis by miR319-targeted TCP4 transcription factor. *Plant Biotechnol. J.* 15: 1284-1294.

Pubmed: [Author and Title](#)

Google Scholar: [Author Only](#) [Title Only](#) [Author and Title](#)

Sundell, D., Street, N.R., Kumar, M., Mellerowicz, E.J., Kucukoglu, M., Johnsson, C., Kumar, V., Mannapperuma, C., Delhomme, N., Nilsson, O., et al. (2017). AspWood: High-Spatial-Resolution Transcriptome Profiles Reveal Uncharacterized Modularity of Wood Formation in *Populus tremula*. *Plant Cell* 29: 1585-1604.

Pubmed: [Author and Title](#)

Google Scholar: [Author Only](#) [Title Only](#) [Author and Title](#)

Tan, Q.K., and Irish, V.F. (2006). The *Arabidopsis* zinc finger-homeodomain genes encode proteins with unique biochemical properties that are coordinately expressed during floral development. *Plant Physiol.* 140: 1095-1108.

Pubmed: [Author and Title](#)

Google Scholar: [Author Only](#) [Title Only](#) [Author and Title](#)

Taylor, G. (2002). *Populus*: arabidopsis for forestry. Do we need a model tree? *Ann. Bot.* 90: 681-689.

Pubmed: [Author and Title](#)

Google Scholar: [Author Only](#) [Title Only](#) [Author and Title](#)

Tischer, S.V., Wunschel, C., Papacek, M., Kleigrewe, K., Hofmann, T., Christmann, A., and Grill, E. (2017). Combinatorial interaction network of abscisic acid receptors and coreceptors from *Arabidopsis thaliana*. *Proc Natl Acad Sci U S A* 114: 10280-10285.

Pubmed: [Author and Title](#)

Google Scholar: [Author Only](#) [Title Only](#) [Author and Title](#)

Tran, L.S., Nakashima, K., Sakuma, Y., Osakabe, Y., Qin, F., Simpson, S.D., Maruyama, K., Fujita, Y., Shinozaki, K., and Yamaguchi-Shinozaki, K. (2007). Co-expression of the stress-inducible zinc finger homeodomain ZFHD1 and NAC transcription factors enhances expression of the ERD1 gene in *Arabidopsis*. *Plant J.* 49: 46-63.

Pubmed: [Author and Title](#)

Google Scholar: [Author Only](#) [Title Only](#) [Author and Title](#)

Tran, L.S., Nakashima, K., Sakuma, Y., Simpson, S.D., Fujita, Y., Maruyama, K., Fujita, M., Seki, M., Shinozaki, K., and Yamaguchi-Shinozaki, K. (2004). Isolation and functional analysis of *Arabidopsis* stress-inducible NAC transcription factors that bind to a drought-responsive cis-element in the early responsive to dehydration stress 1 promoter. *Plant Cell* 16: 2481-2498.

Pubmed: [Author and Title](#)

Google Scholar: [Author Only](#) [Title Only](#) [Author and Title](#)

Tuskan, G.A., Difazio, S., Jansson, S., Bohlmann, J., Grigoriev, I., Hellsten, U., Putnam, N., Ralph, S., Rombauts, S., Salamov, A., et al. (2006). The genome of black cottonwood, *Populus trichocarpa* (Torr. & Gray). *Science* 313: 1596-1604.

Pubmed: [Author and Title](#)

Google Scholar: [Author Only](#) [Title Only](#) [Author and Title](#)

Valdés, A.E., Overnäs, E., Johansson, H., Rada-Iglesias, A., and Engström, P. (2012). The homeodomain-leucine zipper (HD-Zip) class I transcription factors ATHB7 and ATHB12 modulate abscisic acid signalling by regulating protein phosphatase 2C and abscisic acid receptor gene activities. *Plant Mol. Biol.* 80: 405-418.

Pubmed: [Author and Title](#)

Google Scholar: [Author Only](#) [Title Only](#) [Author and Title](#)

Vanzo, E., Jud, W., Li, Z., Albert, A., Domagalska, M.A., Ghirardo, A., Niederbacher, B., Frenzel, J., Beemster, G.T., Asard, H., et al. (2015). Facing the Future: Effects of Short-Term Climate Extremes on Isoprene-Emitting and Nonemitting Poplar. *Plant Physiol.* 169: 560-575.

Pubmed: [Author and Title](#)

Google Scholar: [Author Only](#) [Title Only](#) [Author and Title](#)

von Caemmerer, S., and Farquhar, G.D. (1981). Some relationships between the biochemistry of photosynthesis and the gas exchange of leaves. *Planta* 153: 376-387.

Pubmed: [Author and Title](#)

Google Scholar: [Author Only](#) [Title Only](#) [Author and Title](#)

Wang, L., Hua, D., He, J., Duan, Y., Chen, Z., Hong, X., and Gong, Z. (2011). Auxin Response Factor2 (ARF2) and its regulated homeodomain gene HB33 mediate abscisic acid response in *Arabidopsis*. *PLoS Genet.* 7: e1002172.

Pubmed: [Author and Title](#)

Google Scholar: [Author Only](#) [Title Only](#) [Author and Title](#)

Wang, X., Vignjevic, M., Jiang, D., Jacobsen, S., and Wollenweber, B. (2014). Improved tolerance to drought stress after anthesis due to priming before anthesis in wheat (*Triticum aestivum* L.) var. Vinjett. *J. Exp. Bot.* 65: 6441-6456.

Pubmed: [Author and Title](#)

Google Scholar: [Author Only](#) [Title Only](#) [Author and Title](#)

Warnes, G.R., Bolker, B., Bonebakker, L., Gentleman, R., Huber, W., Liaw, A., Lumley, T., Maechler, M., Magnusson, A., Moeller, S., et al. (2016). gplots: Various R Programming Tools for Plotting Data.

Wickham, H. (2009). *ggplot2: Elegant Graphics for Data Analysis* (Springer-Verlag New York).

Pubmed: [Author and Title](#)

Google Scholar: [Author Only](#) [Title Only](#) [Author and Title](#)

Wildhagen, H., Paul, S., Allwright, M., Smith, H.K., Malinowska, M., Schnabel, S.K., Paulo, M.J., Cattonaro, F., Vendramin, V., Scalabrin, S., et al. (2018). Genes and gene clusters related to genotype and drought-induced variation in saccharification potential, lignin content and wood anatomical traits in *Populus nigra*. *Tree Physiol* 38: 320-339.

Pubmed: [Author and Title](#)

Google Scholar: [Author Only](#) [Title Only](#) [Author and Title](#)

Xu, Z., Zhou, G., and Shimizu, H. (2010). Plant responses to drought and rewatering. *Plant Signal. Behav.* 5: 649-654.

Pubmed: [Author and Title](#)

Google Scholar: [Author Only](#) [Title Only](#) [Author and Title](#)

Yao, W., Zhang, X., Zhou, B., Zhao, K., Li, R., and Jiang, T. (2017). Expression Pattern of ERF Gene Family under Multiple Abiotic Stresses in *Populus simonii* x *P. nigra*. *Front. Plant Sci.* 8: 181.

Pubmed: [Author and Title](#)

Google Scholar: [Author Only](#) [Title Only](#) [Author and Title](#)

Yazaki, J., Galli, M., Kim, A.Y., Nito, K., Aleman, F., Chang, K.N., Carvunis, A.R., Quan, R., Nguyen, H., Song, L., et al. (2016). Mapping transcription factor interactome networks using HaloTag protein arrays. *Proc. Natl. Acad. Sci. USA* 113: E4238-4247.

Pubmed: [Author and Title](#)

Google Scholar: [Author Only](#) [Title Only](#) [Author and Title](#)

Yu, J., Yang, L., Liu, X., Tang, R., Wang, Y., Ge, H., Wu, M., Zhang, J., Zhao, F., Luan, S., et al. (2016). Overexpression of Poplar Pyrabactin Resistance-Like Abscisic Acid Receptors Promotes Abscisic Acid Sensitivity and Drought Resistance in Transgenic Arabidopsis. PLoS One 11: e0168040.

Pubmed: [Author and Title](#)

Google Scholar: [Author Only](#) [Title Only](#) [Author and Title](#)

Zhang, K., and Gan, S.S. (2012). An abscisic acid-AtNAP transcription factor-SAG113 protein phosphatase 2C regulatory chain for controlling dehydration in senescing Arabidopsis leaves. Plant Physiol. 158: 961-969.

Pubmed: [Author and Title](#)

Google Scholar: [Author Only](#) [Title Only](#) [Author and Title](#)

Zhong, S., Shi, H., Xue, C., Wang, L., Xi, Y., Li, J., Quail, P.H., Deng, X.W., and Guo, H. (2012). A molecular framework of light-controlled phytohormone action in Arabidopsis. Curr. Biol. 22: 1530-1535.

Pubmed: [Author and Title](#)

Google Scholar: [Author Only](#) [Title Only](#) [Author and Title](#)